Journal of Surveying and Structural Engineering

Volume No. 11

Issue No. 2

May - August 2023

ENRICHED PUBLICATIONS PVT. LTD

S-9, IInd FLOOR, MLU POCKET,
MANISH ABHINAV PLAZA-II, ABOVE FEDERAL BANK,
PLOT NO-5, SECTOR-5, DWARKA, NEW DELHI, INDIA-110075,
PHONE: - + (91)-(11)-47026006

Journal of Surveying and Structural Engineering

Aims and Scope

Journal of Surveying and Structural Engineering is the major new peer-reviewed journal for building surveyors, structural engineers and other professionals concerned with building condition, defects, valuation, repair and maintenance. The Journal's scope encompasses the diverse range of concerns in the survey, appraisal and valuation of the built environment, including –

1. Building surveys
2. Structural surveys
3. Defect investigation
4. Instrumentation and its use
5. Valuation
6. Repairs and maintenance
7. Dilapidations
8. Fit out and refurbishment
9. Building control and building regulations
10. Party wall issues
11. Remedial works
12. Acquisition surveys
13. Insurance assessment and claims
14. Measured surveys
15. Project management and monitoring
16. Sustainable buildings
17. Dispute resolution
18. Professional liability

Journal of Surveying and Structural Engineering

Journal of Surveying and Structural Engineering

(Volume No. 11, Issue No. 2, May - August 2023)

Contents

Health Monitoring Method for Concrete Slab in Bridge with Functional Declined Bearing

[1] Takayuki Nishido, [2] Shun Imagawa
[1,2]IHI Inspection & Instrumentation Co. Ltd., Yokohama, Japan
E-mail: [1]t_nishido@iic.ihi.co.jp, [2]s_imagawa@iic.ihi.co.jp

ABSTRACT

The functions of movable bearings decline due to corrosion and sediments. As the result, they cannot move or rotate in response to the behaviors of girders. Because of the constraints, the bending moments are generated by the horizontal reaction forces and the heights of girders. Under these conditions, the authors obtained the results by analyses. Tensile stresses due to the moments occurred at temperature fluctuations. The large tensile stress on a concrete slab around the bearings caused cracks. When the widths of cracks increase and steel bars in a concrete slab corrode, the concrete slab may have to be replaced. Even if concrete slabs are newly replaced, cracks will come out again with function declined bearings. By using SOFO sensor that can be fixed with magnets on a steel bridge, it is possible to easily measure the strain of the upper and lower of the web. It is also possible to estimate the stress occurred on the concrete slab from the strain distribution on the girder. Engineers can judge if cracks occur using their results.

Index terms: Bridge bearing, Concrete slab, SOFO sensor, Health monitoring

I. INTRODUCTION

Pin bearings in a simple beam bridge do not produce bending moments at the ends of the beam. The one side of the bearings is also the movable structure to allow expansion and contraction of the bridge due to temperature fluctuations. Because the bearings are made of metal, their functions are often decreased by corrosion and sediments such as soil. The existence of corrosion at the bearings is easily confirmed by visual inspections. However, engineers do not know how much the functions are declined. Therefore the authors examined the effect of the functional decline on the concrete slab of a simple beam bridge with numerical analyses.

A simple composite girder bridge of the length 33.7 m was considered as an example. The bridge made up for four steel plate girders and a concrete slab. The left four bearings were rotatable, and the right four ones were moveable and rotatable. When the movable bearings are constrained, the bending moments generated by the horizontal reaction forces and the heights of the girders cause the concrete slab in tensile stress state. If these stresses are beyond tensile strength of concrete, cracks will occur on the slab. It is generally thought that drying shrinkage of concrete and repeated loading caused cracks in concrete slabs. However, unless engineers restore the function of the bearings, the slab will generate cracks again even if the slab is replaced.

It is difficult to measure the stress occurring on the concrete slab because of the presence of asphalt. Therefore, the SOFO sensor, which is a kind of optical fiber, was considered to measure strains of a steel bridge. We developed a jig to attach the SOFO sensor to the web with a magnet. It can be measured with the same precision as the strain gauge. From the measured strains of the upper and lower of the web, the stress occurring on the concrete slab was calculated by considering strain distribution on the girder. Engineers can judge the possibility of cracking on the concrete slab by the proposed method.

II. FUNCTIONAL DECLINE OF BEARINGS

One of typical bridge bearings is a mechanical device that transmits dead loads and live loads to abutments and piers. As shown in Fig. 1, a simple beam bridge has pinned structure not to produce bending moments in its both ends. Also to allow the expansion and the contraction of the beam due to temperature fluctuations, the one side of the bearings has movable structure.

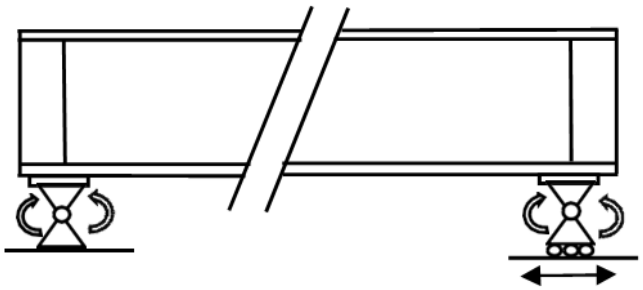

Figure 1: Force transfer function in Bearing

Structure system changes due to the functional declines of bearings. Fig. 2 shows the change of deformation by the decline of movement. The normal bearing moves to absorb the expansion and the contraction of the beam due to temperature. If the right bearing can not move, tensile stresses will occur at the upper side of the concrete slab by the bending moment due to horizontal reaction force as shown in Fig.3. Fig. 4 also shows the change of deformation by the decline of rotation. If the right bearing can not rotate when the live load is applied to the beam, tensile stresses will occur at the right upper side of the slab by the reaction force moment. These stresses are not considered at design stages. If these stressesare larger than tensile strength, then cracks will occur on the slab. It is thought that drying shrinkage, solar radiation and repetition loads by vehicles cause cracks on concrete slabs. However, if engineers do not restore the functions of bearings, there will be the possibility of cracking on the slabs again.

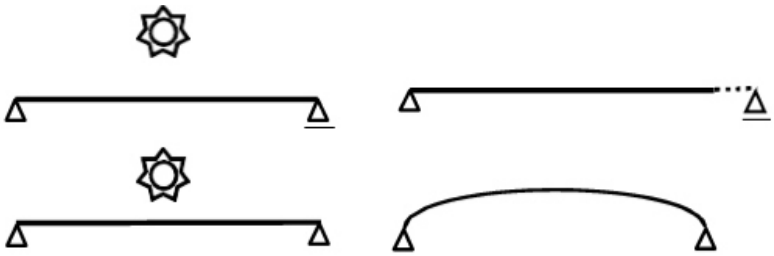

Figure 2: Functional decline on moving in beam

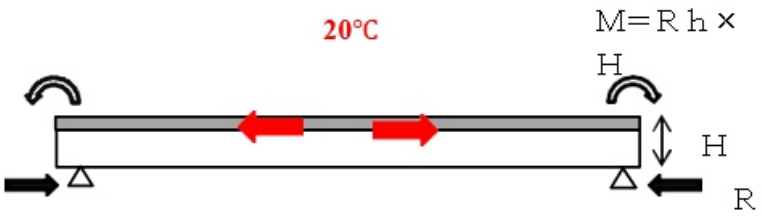

Figure 3: Moment by functional decline

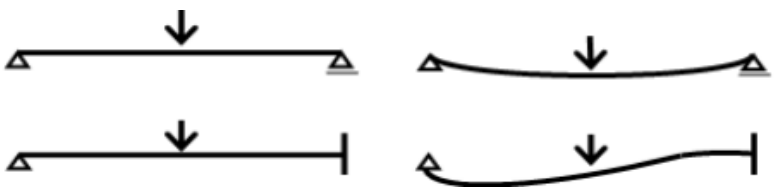

Figure 4: Functional decline on rotation in bridge

III. POSSIBILITY OF CRACKING ON CONCRETE SLAB

We examined the influence of the functional decline on a concrete slab on a simple beam bridge with numerical analyses. The analytical target was a simple composite bridge with its length 33.7m as shown in Fig. 5 and Fig. 6. The concrete slab was placed on the four steel girders in the bridge. The same five crossbeams were put every 5.5 m from the center of the span. As constraint conditions, the bearings on the both sides were rotatable, only the right ones were moveable. The compressive strength of the concrete was defined as 30 N/mm2. The tensile strength of the concrete was 3 N/mm2 by assuming 1/10 of the compression strength. At the arrangement of reinforcing bars in the concrete slab, the main reinforcements with diameters 19mm and the transverse reinforcements with diameters 16mm were placed at intervals of 150mm and 140mm respectively. The width and thickness of the upper flange were 300mm and from 10 to 21mm. Those of the low flange were 480mm and from 9 to 36mm. The widths of flanges are actually changed according to the positions of bridges, but only the thickness of the flange was changed so as to have the same stiffness in this study. The width and thickness of the flanges in the cross beam were 240mm and 10mm respectively.

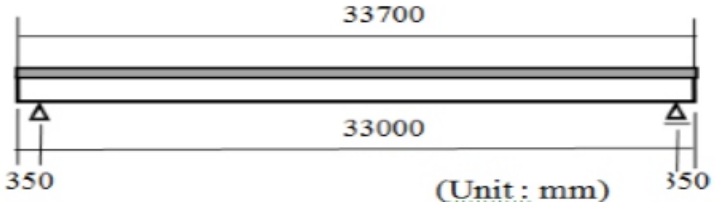

Figure 5: Target simple composite bridge (side view)

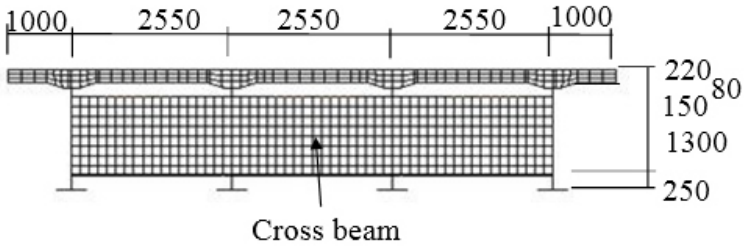

Figure 6: Target simple composite bridge (cross-section view)

The concrete slab and the reinforcing bars were modelled by solid elements and bar elements. The girders and the cross beams were modelled by shell elements. The bearings were not modelled and only the constraint conditions at their positions were given.

Fig. 7 shows FEM model in simple composite bridge. The slab and the girders had same grid points considering their composite condition. Approximate total numbers of the elements and the grids were 101500 and 98000 respectively. Material properties are shown in Table 1. Elastic analyses were done with ABAQUS [1].

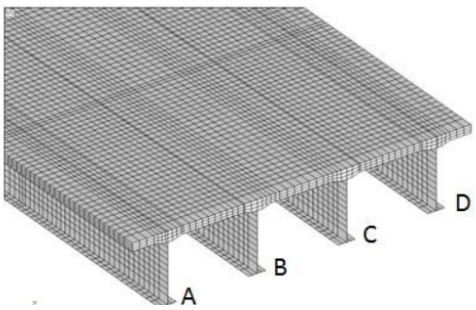

Figure 7: FEM model in simple composite bridge

Table 1

Items	Units	Steel	Concrete
Young'modulus	E N/mm^2	2.0×10^5	2.8×10^4
Shear modulus	G N/mm^2	7.7×10^4	1.2×10^4
Unit weight	ρ kN/m^3	77	23
Poisson'ratio	ν	0.3	0.2
Linear expansion coefficient	α 1/℃	1.2×10^{-5}	1.2×10^{-5}

Table 2 shows analysis conditions. The bearing number is the same as in Fig. 7, focusing on the right side bearings. Here, ○ means free, and × does constraint. The constraint conditions were determined in consideration of the occurrence of the maximum tensile stresses in the concrete slab when temperature loads were applied as shown in Fig. 3. We assumed that girders and the slab have same temperature [2] in a day. The expansion of the girders and the slab are the same at this temperature state on normal bearings. Occurring tensile stresses in the conditions of Table 2 are larger than the ones when there is temperature difference between the girders and the slab. Therefore the temperature load of 20°C was applied to the girders and the slab simultaneously.

As shown in Fig. 4, the constraint conditions were also determined in consideration of the occurrence of the maximum tensile stresses in the concrete slab when the live loads were applied. The reaction force moments occurs when the rotation of the right end is fixed. The moments also occur when the both rotations are fixed. The former moment of the right end is bigger than the latter one. Therefore only the rotation of the right end was fixed.

Specifications for highway bridges [3] prescribe that T-load is used as live load to examine stress on a slab. Therefore three sets of the T-load were applied to the slab as shown in Fig. 8.

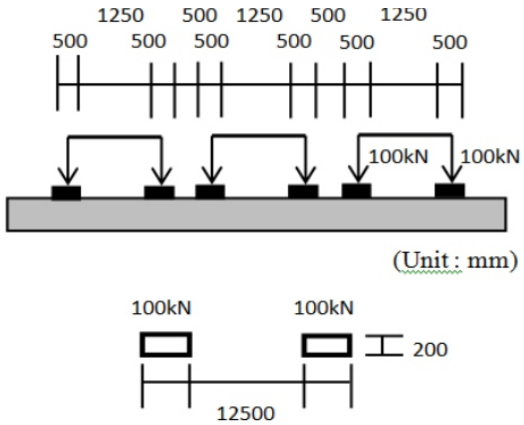

Figure 8: T-load on concrete slab

Table 2

Type	Bearing No.	Movement		Rotation	
		A B	C D	A B	C D
①	C a s e 1	○	○	○	○
Temperature	C a s e 2	×	×	○	○
	C a s e 3	×	○	○	○
②	C a s e 4	○	○	○	○
T-Load	C a s e 5	×	×	×	×
	C a s e 6	×	×	×	○
① + ②	C a s e 7	×	○	○	○

IV. RESULTS

When the bearings functioned normally in Case1, Stresses did not occur on the slab and the girders in beam theory. The transformation and the maximum principal stress on the upper and lower sides of the slab in Case 2 are shown in Fig. 9 and Fig. 10.

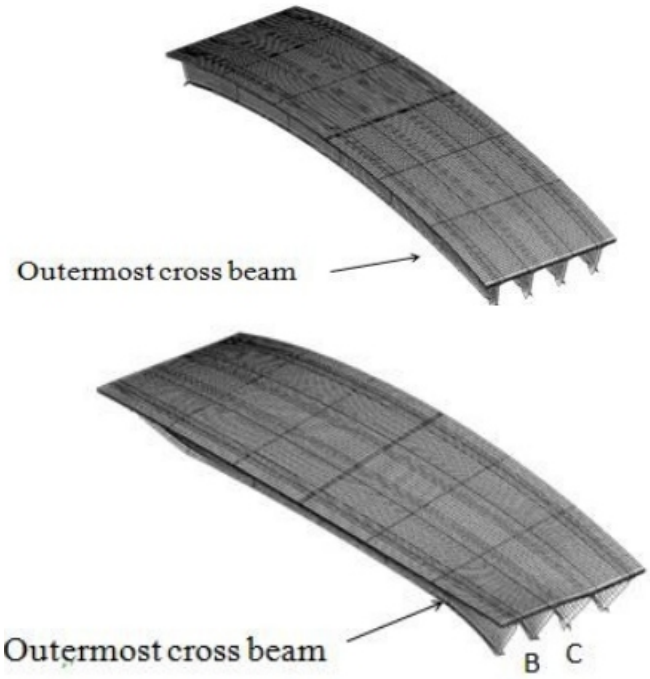

Although the bridge expanded due to the temperature load of 20°C, the movements at the right bearings were fixed. As the bridge was bent on the upper side, the slab could also move. As the result, tensile stresses occurred on the upper side of the slab in this case.

The both ends of the bridge act as pinned supports as shown in Fig. 2. Tensile stresses do not occur at the both ends in beam theory. However only lower flanges were acted as pinned supports in the analysis model, Occurred tensile stresses were about 1.5 N/mm2 between the right bearings and the outermost cross beam. It is thought that tensile stresses on the slab were caused by the bending moments due to the horizontal reaction forces and the girder heights.

The transformation and the maximum principal stress on the upper side of the slab in Case 3 are shown in Fig. 11 and Fig. 12. The slab around the right bearings transformed as like sine-wave. Tensile stresses on the upper and lower sides of the slab were about 2.6 N/mm2 near the movement free bearing B. The large tensile stresses also occurred between the bearings and the outermost cross beam at the right side. Since the constraint conditions were different for the bearings A, B and C, D, the principal stress occurred in the direction of 45 degrees from the bridge axis.

Table 3 shows the maximum tensile stresses in all cases. U means the upper side of the concrete slab. L means the lower side of the concrete slab. The functional declines of the half bearings (A and B) in Case 3 clearly caused larger tensile stresses on the concrete slab than the declines of all bearings from these analyses. The temperature loads also caused larger tensile stresses than the T-loads at the same constraint conditions.

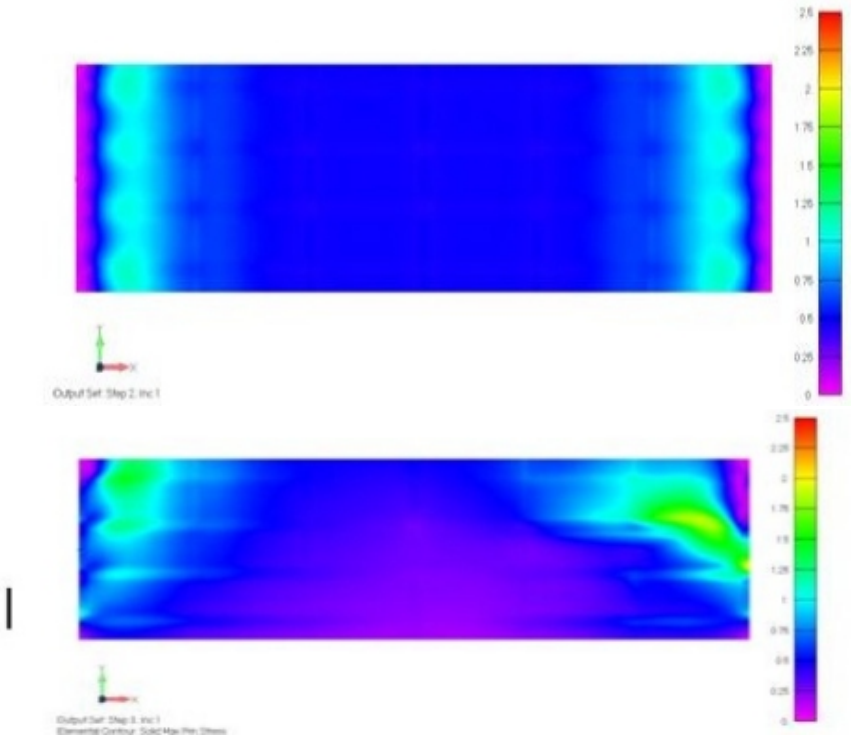

Table 3

Loads	① Temperature				② T-load				① + ②	
Case	1	2	3		4	5	6		7	
Place	U	U	U	L	U	U	U	L	U	L
Stress N/mm^2	0	1.5	2.6	2.6	0	0.3	0.9	1	3.3	3.4

Bridges are actually subject to temperature and live loads simultaneously. Therefore we also thought Case 7 that the temperature load of 20°C and the T-loads were applied to the bridge at the constraint condition of Case 3. The maximum principal stress on the upper side of the slab in case 7 are shown in Fig. 13. Table 3 shows the maximum principal stresses in Case 7. There is also the possibility of cracking on the wide area of the slab in the case.

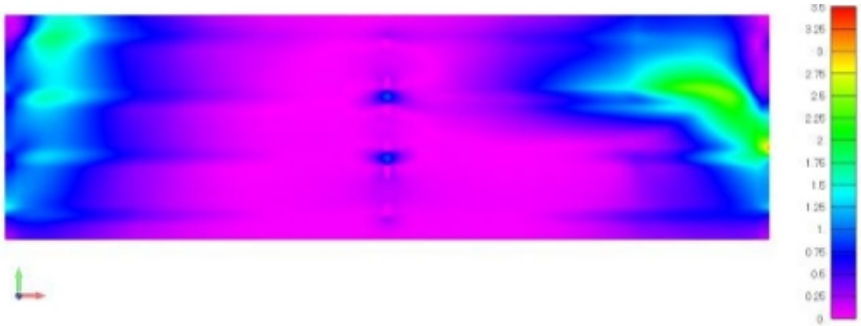

The temperature of an entire bridge became 32°C in measurement results [2]. As the stress in Case 3 in Table 3 is 1.6 times at the temperature, the tensile stress on the slab is 4.2 N/mm2. There is the possibility of cracking in wide area near the bearings. From the results in Table 3, the tensile stresses exceed the allowable stress (3 N/mm2) under the following conditions. There are possibilities that cracks may occur on the concrete slab.

(1) The movements of the all right bearings are constrained (Case 2), and the entire bridge becomes 40 ° C.

(2) The movements of the right bearings C and D are constrained (Case 3), and the entire bridge becomes 23 ° C.
(3) The movements of the right side bearings C and D are constrained (Case 3), and the T load and the entire bridge becomes 18 ° C. Although it cannot be superimposed in this case, it is a prediction with reference to Case 3.

V. CONFIRMATION OF GENERATED STRESS ON CONCRETE SLAB

From the analyses, cracks may occur on the upper and lower sides of the slab when a bridge, which have functional decline of bearings, expand or contract with temperature fluctuations. However, it is difficult to measure the stress occurring on the concrete slab because of the presence of asphalt.

If loads act on a bridge, stress is occurred inside the bridge. Stress and strain are in a proportional relation. The strain is assumed to be a linear distribution in the height direction of the girder on the compound bridge. For this reason, the strain on the concrete slab can be estimated using the strains at the upper and lower of the web. The stress occurred on the concrete slab is calculated by multiplying the strain by the Young's modulus. For strain measurement, a strain gauge is generally used. In the case, it is necessary for the strain gauge to peel off paint at the measurement location. It is also necessary to paste the gauge with an adhesive. When measuring is continued at intervals of once a month for example, gauge protections on the surface also required.

Therefore, we considered a method to confirm the stress occurred on the concrete slab easily using a SOFO sensor (Surveillance d'Ouvrages par Fibres Optiques). SOFO sensor is a measuring displacement system using optical fiber cables. It is composed of two optical fibers as shown in Fig. 14. As the measuring fiber is added tension force in advance, it expands and contracts in response to the deformation between two points fixed at structures. The other is the reference fiber in spiral, of which length is not affected by the deformation between the fixed points. The SOFO sensor measures the difference between the two optical fibers. Strains can also be calculated from deformation results.

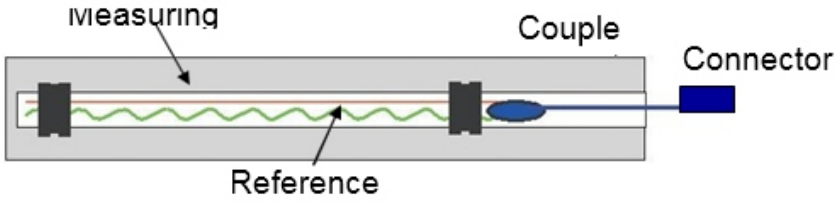

Figure 14: Structure of SOFO sensor

In order to measure the strains from the deformations of a painted steel bridge, jigs were made to attach the SOFO sensor to the web with a magnet. It is not necessary to peel off paint for measurement or paste with adhesive. By installing the SOFO sensor at the same position on the web, it is easy to measure strains once a month for example. The jig is shown in Fig. 15. The attraction force of the magnet is 454 N, the weight of a jig is 3.4 kg, and its size is 147 × 72 × 108 mm respectively. The jig can make fine adjustments for the SOFO sensor in the front and back direction.

Figure 15: Jig with magnet for SOFO sensor

It is necessary to confirm that the jigs do not shift during measurement. The states of tension and bending, which are acting on an actual bridge, were considered. Loading tests were conducted on a painted flat plate and an H-shaped girder. The flat plate was used for a tensile test, and the H-shaped girder was used for a four-point bending test.

As shown in Fig. 15, strain gauges were attached and SOFO sensor with 300 mm length was set. The both strain values were compared. Fig. 16 and Fig. 17 show the results of the load tests on the flat plate and the H-shape girder. Loading was repeated 3 times for both tests. In the four-point bending test, the influence of the offset for the SOFO sensor was considered. From these results, it was found that the SOFO sensor could be measured with the same precision as the strain gauge without shifting jigs during the loading tests.

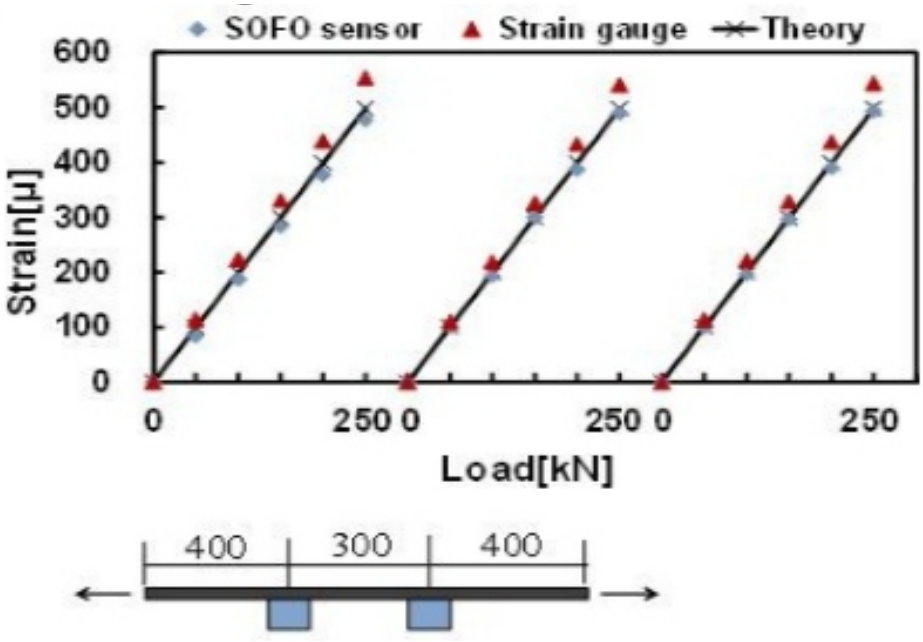

Figure 16: Result of load test on flat plate

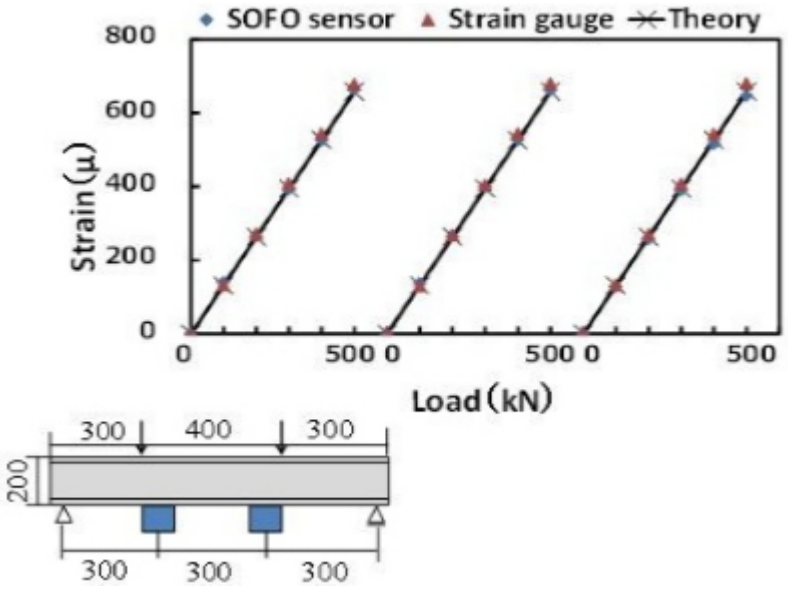

Figure 17: Result of load test on H-shaped girder

In an actual bridge, the SOFO sensors with magnets are attached to the upper and lower of the web near the bearing. From the analyses results, for Case 2 and Case 3 where temperature fluctuations were greatly affected, the strain distributions by the proposed method and by the analysis are shown in Fig. 17 and Fig. 18 respectively.

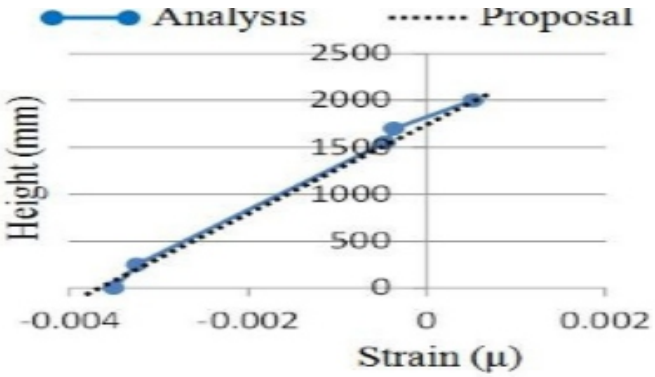

Figure 18: Strain distribution in Case 2

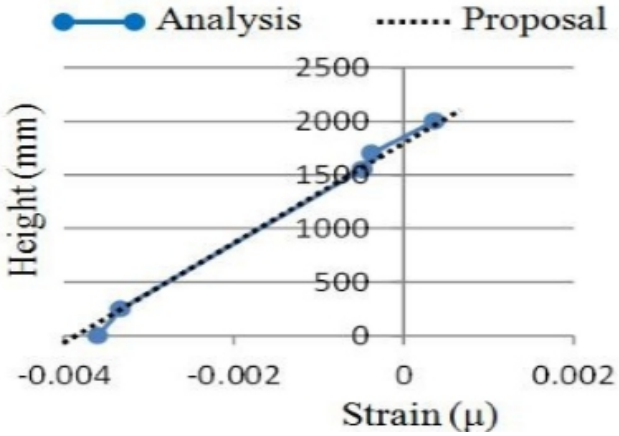

Figure 19: Strain distribution in Case 3

Table 4 shows the stresses occurred on the upper surface of the concrete slab for the both cases. In Case 2, it is possible to judge that cracks occur in the concrete slab when the tensile stress obtained by the proposed method is 4.11 N/mm2 or more. The judgment is on the safety side based on the error.

Table 4

	Stress (N/mm^2)		
Case No.	**① Analysis**	**② Proposal**	**Error ②/①**
Case2	1.01	1.39	1.37
Case3	1.46	1.39	0.95

CONCLUSION

From the results of the analyses and the measurements, the following findings are obtained.

(1) The functional decline of bearings causes cracking on concrete slabs to which temperature loads and live loads are applied.

(2) If the function of bearings is not restored, cracks may occur on the slabs again after the replacements of the ones.

(3) The SOFO sensors are easily attached to the upper and lower of a web with magnets. As the stress occurred on the upper and lower of the concrete slab can be calculated from the obtained strains, Engineers can estimate the possibility of cracking.

REFERENCES

[1] ABAUS Inc., ABAQUS analysis user's manual, version 6.10-1, 2010.

[2] K. Yamamura and S. Iwasaki et al., "Actual situation and examination of deformation behavior of existing composition I girder with the temperature variation," Proc. Northeast Branch conf. of JSCE, I-26, 2010.

[3] Japan Road Association, Design Specifications for Highway Bridges, 2012.

[4] A. Othonos and K. Kalli, Fiber Bragg Grating, Artech House Publishers, pp. 95-99. 1999.

Seismic Non- Linear Time History Analysis of Multi Storied RCC Residential Building Subjected to Different Earthquake Ground Motions using ETABS

1 Abdul Ahad Faizan, 2 Osman Kirtel

[1]PhD Student, Civil Eng. Department, Institute of Graduate Education, Sakarya University of Applied Sciences, Sakarya , Turkey

[2]Assistant Professor, Civil Eng. Department, Institute of Graduate Education, Sakarya University of Applied Sciences, Sakarya , Turkey

E-mail: [1]ab.ahad_faizan@yahoo.com, [2]okirtel@sakarya.edu.tr

A B S T R A C T

Seismic analysis of reinforced Concrete (RCC) buildings are one of the research interests nowadays and it is because of, earthquake causes lots of damage and losses with respect to life and damage of structures. The present study is limited to reinforced concrete multi-storied residential building under influence of three different earthquake ground motions. In this study, a nonlinear time history analysis is performed on eight storey RCC building frame considering time history of Landers earthquake 1992, Kobe earthquake 1995 and ChiChi earthquake 1999 using ETABS software. Analysis also performed to study the behavior of building under the seismic and gravity loads as per the IS-1893:2002. All analysis are compared for outcomes such as storey displacements and base shears. From the study it is recommended that analysis of multistoried RCC building using Time History method becomes necessary to ensure safety against earthquake force.

Keywords - Time History Analysis, Multistoried RCC Building, ETABS, IS-1893:2002, Storey Drifts, Storey Displacements, Base Shear.

I. INTRODUCTION

And All over world, there is high demand for construction of tall buildings due to increasing urbanization and spiraling population, and earthquakes have the potential for causing the greatest damages to those tall structures. Since earthquake forces are random in nature and unpredictable, the engineering tools need to be sharpened for analyzing structures under the action of these forces. When earthquakes occur, a building undergoes dynamic motion. This is because the building is subjected to inertia forces that act in opposite direction to the acceleration of earthquake excitations. These inertia forces, called seismic loads, are usually dealt with by assuming forces external to the building. So apart from gravity loads, the structure will experience dominant lateral forces of considerable magnitude during earthquake shaking. It is essential to estimate and specify these lateral forces on the structure in order to design the structure to resist an earthquake. Earthquake loads are required to be carefully modeled so as to assess the real behavior of structure with a clear understanding that damage is expected but it should be regulated. Analyzing the structure for various earthquake intensities and checking for multiple criteria at each level has become an essential exercise for the last couple of decades.

For determination of seismic responses it is necessary to carry out seismic analysis of the structure using different available methods (1). Static Analysis, (2) Nonlinear Static Analysis, (3) Linear Dynamic Analysis; and (4) Nonlinear Dynamic Analysis. Linear static analysis or equivalent static method can be used for regular structure with limited height. Linear dynamic analysis can be performed by response spectrum method. The significant difference between linear static and linear dynamic analysis is the

level of the forces and their distribution along the height of structure. Nonlinear static analysis is an improvement over linear static or dynamic analysis in the sense that it allows inelastic behavior of structure. A nonlinear dynamic analysis is the only method to describe the actual behavior of a structure during an earthquake. The method is based on the direct numerical integration of the differential equations of motion by considering the elasto-plastic deformation of the structural element.

Reinforced concrete buildings have been damaged on a very large scale in Landers, Kobe and ChiChi earthquakes, Even though these buildings are analyzed and designed as per IS code. The damages are caused by inconsistence seismic response, irregularity in mass and plan, soft storey and floating columns etc. Hence it becomes necessary to evaluate actual seismic performance of building subjected to earthquake forces. Time History analysis gives more realistic seismic behavior of the building. It gives more accurately seismic responses than response spectrum analysis because of it incorporates material nonlinearity and dynamic nature of earthquake.

II.LITERATURE REVIEW

Patil A. S. (5) studied nonlinear dynamic analysis of 10 storied RCC building considering different seismic intensities and also studied seismic response of such building. The building under consideration is modeled with the help of SAP 2000-15 software and 5 different time histories have been used. The result of the study shows similar variations pattern in seismic response such as base shear and storey displacements and concluded that time history is realistic method used for seismic analysis. It provides a better check to the safety of structure analyzed and designed.

Bhagwat et al. (6) studied dynamic analysis of G+12 multistoried practiced RCC building considering for Koyna and Bhuj earthquake is carried out. The Time History Analysis and Response Spectrum Analysis and seismic responses of the building are comparatively studied. The modeled with the help of ETABS9.7.2 software. Two time histories (i.e. Koyna and Bhuj) have been used to develop different criteria (base shear, storey displacement, storey shear), and concluded that, the value of base shear for Bhuj earthquake is 49.11% more than the Koyna earthquake, and Response Spectrum method gives 50% more result than Time History Analysis.

Dubey et al. (7) presented design of multistoried irregular building with 20 stories and modeled it using software STAAD-PRO for seismic zone IV in India, dynamic response of building under actual earthquake, DELINA (ALASKA)2000 have been considered. This paper highlights the comparison of Time History Method and Response Spectrum Method. The story displacement result has been obtained by using both method of dynamic analysis, and Concluded that Time History Analysis is found to be 2 to 8% higher than that of Response Spectrum Analysis in both type of building i.e. regular and irregular, For high rise building it is necessary to provide dynamic analysis because of nonlinear distribution of force. Storey displacement is found greater in THM as compared to RSM, and observed that the base shear is greater in RSM compared to THM. Thus it can be concluded that time history analysis is economically better for designing.

Rampure et al. (8) studied the dynamic time history analysis and response spectrum analysis of a concrete gravity dam by using STAAD-PRO. Finite element approach is used to analyze the dam and a concrete gravity dam model is prepared in STAAD-PRO to perform the time history analysis and response spectrum analysis and comparison is done between both these methods. They concluded that STAAD-PRO is most convenient and less tedious for dynamic analyses and it provides a computing

environment to investigate modelling assumption and computational processes related to the static and seismic structural stability of gravity dam. It is necessary to analyze the structure by dynamic analysis of both these method for below the height of dam 100m and above the height of dam 100m. Hawaldar et al. (9) presented G+12 storey building model with and without infill the time history analysis used for Bhuj and Koynaearthquake function it is carried out in ETABS 2013 software. The seismic responses of story displacements, storey drifts are observed. Time history plots of base force v/s time and roof displacement v/s time for both time history functions are compared and studied. They concluded that the displacement values for bhuj function are higher than the displacement value for koyna function and those for infill building are less than that without in filled building and drift value of bhuj function were more in comparison with drifts for koyna function and infill drift values are comparatively less than for without infill drift values for both time history function. Harshita et al. (10) studied the dynamic behavior of multistoried symmetrical building frame using IS1893- 2002 code recommended response spectrum method and time history method. Study focuses to evaluate the base shear, response spectra at different story levels, bending moment diagram, shear force diagram variation in the building. Analysis has been carried out using the STAAD-PRO software based on the matrix analysis. Based on the result it is found that the base shear obtained from time history analysis is slightly higher compared to response spectrum analysis, this may be due to variation in amplitude and frequency content of the ground motion.

III. OBJECTIVES

The main objective of the present study is to carry out the seismic response of 8 storey RCC frame structure using time history analysis methods. The specific objectives are as given below:

1. Seismic non-linear time history analysis of multi-storied RCC building under influence of different earthquakes using Etabs.
2. To study the behavior of multi-storied RCC building under the action of load combination (seismic loads and gravity loads).
3. The time history analysis is performed for the RCC building firstly and then the seismic analysis is performed for load combination (DL, LL, and EQL).
4. Analysis of base shear and displacement on different storey.
5. To compare seismic behavior of multistoried RCC framed building for different earthquakes in terms of various responses such as, base shear and displacements.
6. The entire process of modeling and analysis of all the primary elements for all the models are carried by using ETABS 2016 nonlinear version software.

IV. RESEARCH METHODOLOGY

Non-linear time history and load combination analyses performed as per the IS-1893-2002 (11). The finite element analysis software ETABS Ultimate 2016 (12) is utilized to create 3D model and run all analyses. The software is able to predict the geometric nonlinear behaviour of space frames under static or dynamic loadings, taking into account both geometric nonlinearity and material inelasticity. The software accepts static loads (either forces or displacements) as well as dynamic (accelerations) actions and has the ability to perform Eigen values, nonlinear static pushover and nonlinear dynamic analyses.

V. PROBLEM FORMULATION

Various time histories are considered as a real time seismic data to perform ETABS analysis. The time histories are: Landers, Kobe and Chichi. Several data's are to be decided to use as an input parameters for software analysis. The parameters are tabulated in tabular format.

Preliminary Data	
Project type	8 storey Residential Building
Dimension of building	19.10m x 16.70m
Beam size	35cm x 40cm
Column size	35cm x 35cm
Slab thickness	15cm
Support Condition	Fixed
G+Typical storey height	3m
Underground storey height	4m
Live load, LL	2kN/m²
Partition and floor finishing load, FL	1kN/m2
External Wall load	13kN/m
Grade of concrete	M30
Seismic zone	III
Zone factor	0.16
Response reduction factor R	3
Importance factor	1
Damping	5%

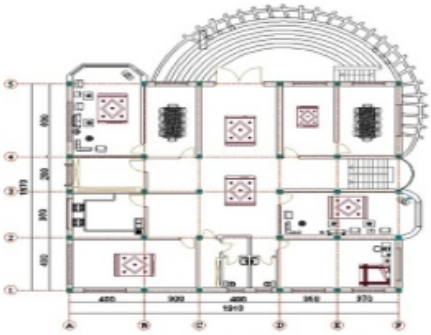

a) Architectural plan

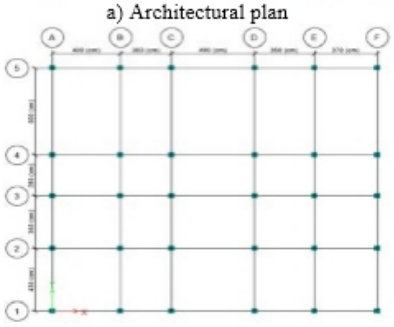

b) 3D view of residential building (Revit Architecture)

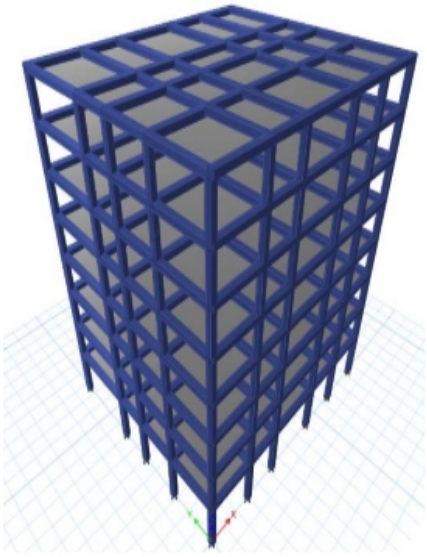

d) 3D view of residential building (ETABS)

Fig.1: Layout of multi-storied RCC residential building

VI. ANALYSIS OF STRUCTURE

TIME HISTORY ANALYSIS

Various time histories are considered as a real time seismic data to perform ETABS analysis. Several data's are to be decided to use as an input parameters for software analysis. In this study, a nonlinear time history analysis will be performed on a multi storey RCC building frame considering time history of Landers Earthquake 1992, Kobe Earthquake 1995 and ChiChi Earthquakes 1999.

The refined and convenient special purpose analysis and design program Etabs is used to create 3D model and run all analyses. The software is able to predict the geometric nonlinear behavior of space frames under static or dynamic loadings, taking into account both geometric nonlinearity and material inelasticity. Figure 2. shows the details of acceleration time history of Landers, Kobe and Kocaeli Earthquakes. Results obtained from the analysis are tabulated in Tables 1 to 7. Graphical representations of variations in results are shown in Figures 3 to 9.

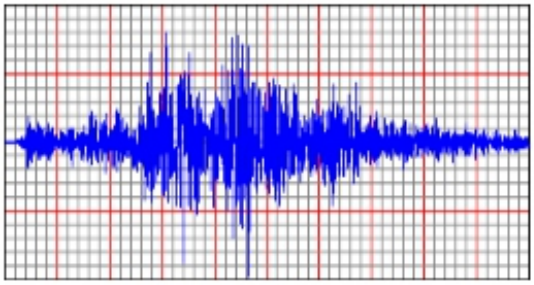

Details of Landers time history
Max. P.G.A: 0.78g
Duration: 30 sec

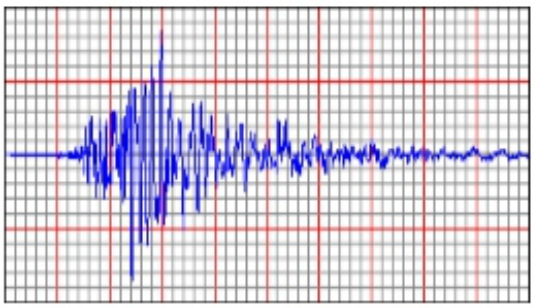

Details of Kobe time history
Max. P.G.A: 0.50g
Duration: 30 sec

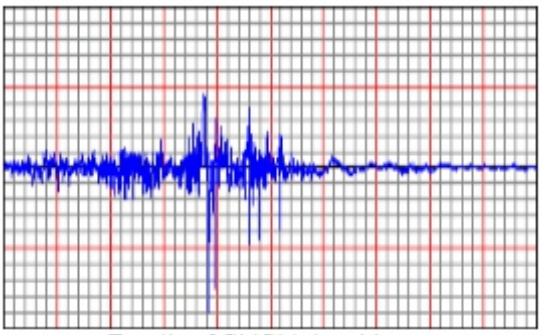

Details of ChiChi time history
Max. P.G.A: 0.36g
Duration: 30 sec

Fig. 2: Details of acceleration time history for different earthquakes

Maximum Base Shear

The base shear of a RCC building is calculated by time history analysis method. In the time history analysis of a building Landers earthquake 1992, Kobe earthquake 1995 and ChiChi earthquake 1999 earthquake records are used. The numerical value of the building are given in Table 1 and shown as graphic form (Fig.3).

Maximum Base Shear (abs)					
Time History	**P.G.A (g)**	**Fx (kN)**	**Fy (kN)**	**Mx (kN.m)**	**My (kN.m)**
Landers	0.78	4065.02	4136.37	64906.53	65716.67
Kobe	0.5	3938.64	3507.05	63849.95	65460.58
ChiChi	0.36	3474.74	3437.3	54048.43	55000.06

Table 1: Maximum base reaction of building for different earthquakes

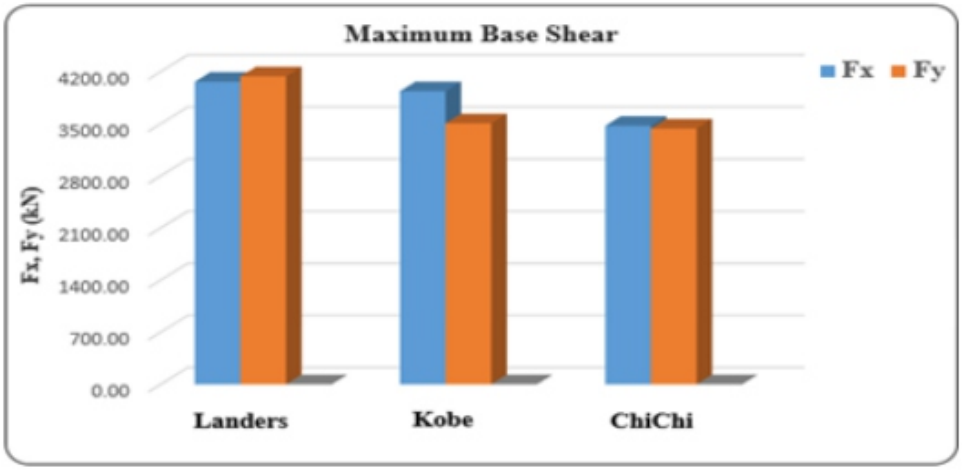

Fig. 3: Storey base shear

The Fig.3 shows the comparison of absolute base shear for RCC building under influence of different earthquake ground motions. From the analysis it observed that, the base share for Landers earthquake is bigger than Kobe earthquake and ChiChi earthquake respectively.

Absolute Storey Displacements

The displacement of RCC building is calculated by time history analysis method. The maximum values of absolute storey displacements of 8 floor RCC building for different earthquakes in x and y directions are given in Table 2 and Table 3. The numerical value which is got from analysis is also shown as graphic form (Fig. 4, Fig. 5).

	Storey Max Displacements for X Direction		
Storey	**Landers (0.78g)**	**Kobe (0.50g)**	**ChiChi (0.36g)**
Storey 8	120.4	119.44	99.7
Storey 7	115	113.33	96.6
Storey 6	105.73	102.91	91.12
Storey 5	95.82	89.32	83.09
Storey 4	84.73	74.06	72.46
Storey 3	69.44	58.28	59.47
Storey 2	51.64	42.81	44.5
Storey 1	32.19	26.3	27.68

Table 2: Storey max displacements for x direction

	Storey Max Displacements for Y Direction		
Storey	Landers (0.78g)	Kobe (0.50g)	ChiChi (0.36g)
Storey 8	130.12	118.52	104.71
Storey 7	123.95	112.82	101.24
Storey 6	113.53	103.83	95.35
Storey 5	100.28	91.74	86.88
Storey 4	86.84	77.48	75.76
Storey 3	70.84	61.77	62.15
Storey 2	54.63	45.11	46.49
Storey 1	34.89	27.38	28.67

Table 3: Storey max displacements for y direction

The Fig.4 and Fig. 5 shows the comparison of displacement for RCC building under influence of different earthquake ground motions in x and y directions. From the analysis it observed that, the floor maximum displacement for Landers earthquake is bigger than Kobe earthquake and ChiChi earthquake respectively.

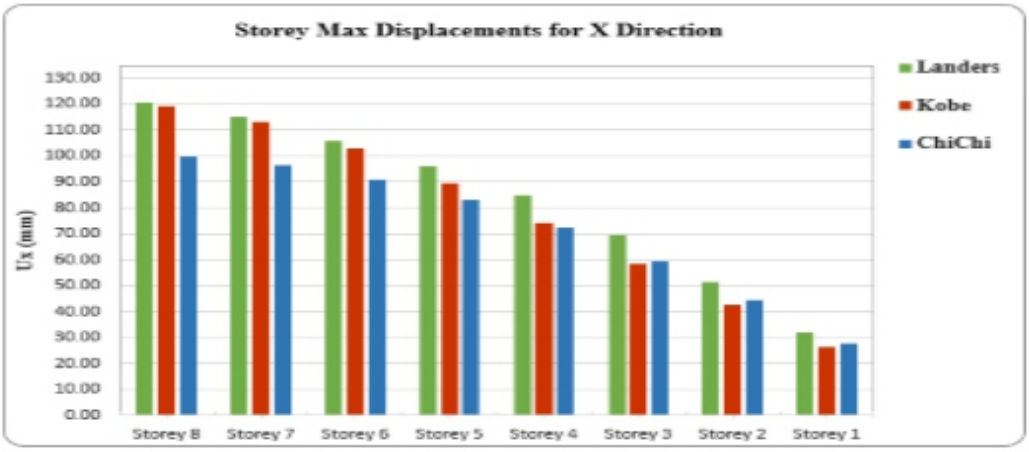

Fig. 4: Storey max displacement

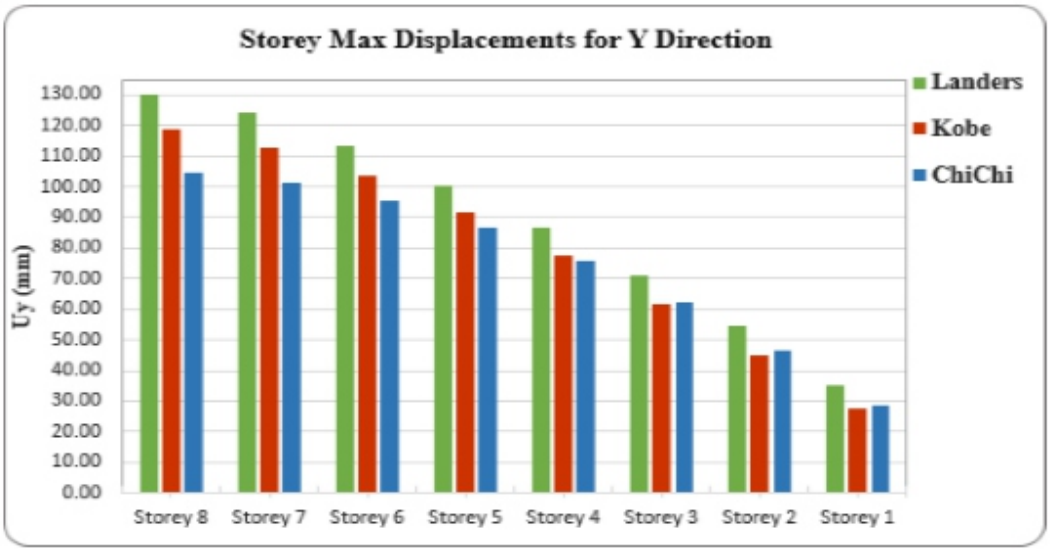

Fig. 5: Storey max displacement

6.2. LOAD COMBINATION ANALAYSIS

There are two types of load considered in this structural analysis. They are gravity loads that include dead load and live load, and earthquake loads. Results obtained from the analysis are tabulated in Tables 8 to 11. Graphical representations of variations in results are shown in Figures 10 to 12.

A)Gravity Loads

Dead loads and live loads are defined as gravity loads that will be accelerated laterally with the structural frame under earthquake motion. Live loads are defined as gravity loads that do not accelerate laterally at the same rate as the structural frame when the structure under goes earthquake motion.

B) Earthquake Load

Earthquake load consists of the inertial forces of the building mass that result from the shaking of its foundation by a seismic disturbance. Other severe earthquake forces may exist, such as those due to land sliding, subsidence, active faulting below the foundation, or liquefaction of the local subgrade as a result of vibration.

C)Load Combinations

The various loads should, therefore, be combined in accordance with the stipulations in the relevant design codes. In the absence of such recommendations, the following loading combinations are made. The most unfavorable effect in the building, and structural member concerned may be adopted. It should also be recognized in load combinations that the simultaneously occurrence of maximum values of earthquake and imposed loads. Load combination analysis performed to study the behavior of building under the seismic and gravity loads as per the IS-1893-2002.

Base Reactions

The maximum values of base reaction of 8 floor RCC frame from base for earthquake load and gravity loads (live load and dead load) are given in Table 8.

Maximum Base Shear Results for Different Load Combinations (abs)			
Load Case	**Fx (kN)**	**Fy (kN)**	**Fz (kN)**
1.5DL+1.5LL	0	0	64961.78
1.2DL+1.2LL+1.2EQL	9765.85	958.48	51969.43
Maximum Base Shear Results for Different Load Combinations (abs)			
Load Case	Mx (kN.m)	My (kN.m)	Mz (kN.m)
1.5DL+1.5LL	533658.96	620739.83	0
1.2DL+1.2LL+1.2EQL	445883.21	689733.97	78253.23

Table 8. Max base shear results for diff. load combinations

Storey Displacements for 1.5DL+1.5LL

The maximum values of absolute storey displacements of 8 floor RCC building for live load and dead load combination are given in Table 9.

Storey Max Displacements for 1.5DL+1.5LL		
Story	**Load Case**	**Uz (mm)**
Storey 8	1.5DL+1.5LL	13.21
Storey 7	1.5DL+1.5LL	12
Storey 6	1.5DL+1.5LL	11.7
Storey 5	1.5DL+1.5LL	10.97
Storey 4	1.5DL+1.5LL	10.04
Storey 3	1.5DL+1.5LL	8.87
Storey 2	1.5DL+1.5LL	7.42
Storey 1	1.5DL+1.5LL	6.06

Table 9. Max displacements for 1.5DL+1.5LL

Storey Displacement 1.2DL+1.2LL+1.2EQL

The maximum values of absolute storey displacements of 8 floor frame for seismic load and gravity loads (live load and dead load) combination in both x and y directions are given in Table 10 .

Storey Max Displacements for 1.2DL+1.2LL+1.2EQL		
Story	**Ux (mm)**	**Uy (mm)**
Storey 8	361.84	76.7
Storey 7	344	72.92
Storey 6	314.65	66.58
Storey 5	276.5	58.39
Storey 4	232.22	48.91
Storey 3	184.03	38.62
Storey 2	133.71	27.91
Storey 1	81.38	16.82

Table 10: Max displacements for 1.2DL+1.2LL+1.2EQL

VII. CONCLUSIONS

Seismic non-linear time history analysis of a multistoried RC building for three different earthquakes; Landers, Kobe and ChiChi is carried out. From the present study the following conclusions can be drawn out.

1. The seismic responses namely base shear, and storey displacements in both the directions (x, y) are found for the Landers time histories (0.78g), Kobe time histories (0.50g) and ChiChi time histories (0.36g).
1. From results it is observed that the storey shear is decreased as height of the building increased and reduced at top floor in all the building modelssubjected to seismic loads considered. The storey shear is maximum at the base.
2. The base shear of structure increases as we go to time histories with higher PGA. For the proposed RC building the base shear (x and y directions) value of Lander time history is 4065.02 KN, 4136.37 KN for Kobe time history is 3938.64 KN, 3507.05KN and for ChiChi time history is 3474.74 KN, 3437.30KN . This means base shear increases if PGA is changes from 0.78g to 0.50g and 0.36g.
3. The displacement of building models increases with the increasing of time history PGA. The displacement is very high at roof and very low at the base. The displacements in both directions (x, y) occurs at top floor for Landers earthquake is 120.40mm, 130.12mm; Kobe earthquake is

119.44mm, 118.52mm and ChiChi earthquake is 99.70mm, 104.71mm. This means top floor displacement increases if PGA is changes from 0.78g to 0.50g and 0.36g.

4. The values of base shear, storey displacements and storey drifts (X direction) for Landers time history are found to be more by 1.03, 1.16; 1.01, 1.20; 1.05, 1.16 times, respectively as compared to Kobe time histories and ChiChi time histories.
5. The values of base shear and storey displacements (y direction) for Landers time history are found to be more by 1.18, 1.20; 1.24; 1.20 times, respectively as compared to Kobe time histories and ChiChi time histories.
6. It is concluded from results and discussion that the outcomes varies from time history to time history. The designers worked for seismic zones must consider time history data while designing RC buildings.
7. As time history is realistic method, used for seismic analysis, it provides a better check to the safety of structures analyzed and designed by method specified by IS code.
8. Results from various time histories can be efficiently presented and utilized for future building design problems. Standards can be established for same.
9. For important structures time history analysis should be performed as it predicts the structural response more accurately in comparison with other methods.

REFERENCES

[1] Duggal S K (2010), "Earthquake Resistance Design of Structure", Fourth Edition, Oxford University Press, New Delhi.

[2] Haselton C B and Whittaker A S (2012), "Selecting and Scaling Earthquake Ground Motions for Performing Response-History Analyses", The 15th World Conference on Earthquake Engineering.

[3] Romy M and Prabha C (2011), "Dynamic Analysis of RCC Buildings with Shear Wall", International Journal of Earth Sciences and Engineering, ISSN 0974- 5904, Vol. 04, 659-662.

[4] Shaha V and Karve S (2010), "Illustrated Design of Reinforced Concrete Buildings", Sixth Edition, Structures Publication, Pune.

[5] Patil A.S, Kumbhar P.D, "Time history analysis of multistoried RRC building for different seismic intensities", International Journal of Structural and Civil Engineering Research, vol.-02, issue-03, Aug 2013.

[6] Bhagwat Mayuri D, "Comparative study of Performance of multistoried building for Koyna and Bhuj earthquake by THM and RSM", International Journal of Advanced Technology in Engineering and Science, vol.no.-02, issue- 07, ISSN: 2348-7550, July 2014.

[7] Dubey S.K, Sangamnerka Prakash, Agrawal Ankit, "Dynamic analysis of structures subjected to earthquake load", International Journal of Advance Engineering and Research Development, vol.-02, issue-09, ISSN: 2348-4470, Sep.2015.

[8] Rampure Aarti baburao, "Comparison between Response Spectrum Method and Time History Method of dynamic analysis of concrete gravity dam", Open Journal of Civil Engineering,June 2016.

[9] Hawaldar Jyothi C, "Earthquake analysis of G+12storey building with and without infill for Bhuj and Koyna earthquake function", International Research Journal of Engineering and Technology(IRJET), vol.-2, issue-05,ISSN:2395-0056, august 2015.

[10] Harshita, "seismic Analysis of symmetric RC frame using RSM and THM", International Journal of Scientific Research and Education, vol-02, issue-03, march 2014.

[11] IS 1893 (Part 1):2002 Design Criteria for Earthquake Resistant design of Structure.

[12] CSI, (2016), extended 3D analysis of building structures (ETABS), Computers and Structures Inc., USA.

Studying the Effect of Elevated Temperatures on A Designed RC Structure of A Hotel

[1]Hamza Hamida, [2]Anas Demyati, [3]Al- Hassan Maghrabi, [4]Mohammed Al- Osta

[1]Construction Engineering and Management Department, KFUPM, Dhahran, Saudi Arabia

[2, 3, 4]Civil and Environmental Engineering Department, KFUPM, Dhahran, Saudi Arabia

E-mail: [1]g201215140@kfupm.edu.sa, [2]s201254700@kfupm.edu.sa, [3]s201224980@kfupm.edu.sa, [4]malosta@kfupm.edu.sa

ABSTRACT

The purpose of this research paper was to design and analyze a five-story hotel building. The structure of the building was designed using cast in place reinforced concrete members, and two different slab systems (solid slabs and flat slabs). Both systems were subjected to high temperatures in different sections of the building. The effect of high temperatures on the redistribution of stresses was studied and analyzed. The structural design for both systems was performed according to local and international standards. Specific data related to conducted experimental researches was considered to be used in the study of the effect of elevated temperatures on the structural systems. The adopted software in the structural analysis and design was STAAD PRO. It was used to study the effect of elevated temperatures on the behavior both structural systems by observing the change in the required area of steel for specific structural elements located at different locations. The results revealed that the obtained design for both structural systems from STAAD PRO is safe. Moreover, the behavior of both structural systems under elevated temperature conditions indicates that the location of a structural element and the type of the applied temperature load are the major factors affecting the redistribution of the stresses and convert structures from safe to unsafe.

Keywords- Reinforced Concrete Structure, Elevated Temperatures, STAAD PRO, Solid Slabs, Flat Slabs.

I. INTRODUCTION

Reinforced concrete (RC) structures are the most common type of structures that are used nowadays. RC is used for the construction of buildings, bridges, dams and tunnels. Many types of buildings, such as residential, commercial, institutional, and educational buildings are reinforced concrete structures. Tourism is an essential part for many countries around the world from both the economic and cultural point of views. Therefore, hotels are available in major and minor cities within a country in order to accommodate tourists and people who are foreigners to the city. However, there are certain environmental conditions or accidents might affect the durability of reinforced concrete structures such as high temperatures. High temperatures or fires may affect the properties of different types of materials. The purpose of research paper was to design and analyze two different structural systems for a hotel building, which are solid slab and flat slab properly to resist dead, live, wind and other types of loads and then to study the effect of elevated temperatures on both structural systems using data related to conducted research experiments in order to determine the structural behavior under these conditions. The hotel is a five-story building with a total height of 23.8 meters. Each floor has a height of 3.3 meters.

II.LITERATURE REVIEW

Background

Steel is highly affected by high temperatures and its properties can widely change based on its temperature. Although concrete has more resistance to high temperatures, it is not immune to it.

Reinforced concrete is composed of concrete and steel reinforcing bars. The main components of concrete are cement paste and aggregates. The studied effects of high temperature on each of these components will be reviewed and described in the following sections.

Effect of High Temperature on Concrete Under high temperature, all the hydration products in the cement paste start to decompose. These decompositions result in changes in volume and stiffness of the cement paste which result in cracks and voids that significantly damage the concrete mix. The effect on concrete properties is associated with the type of aggregate used in the concrete mixture. The classification of aggregates is generally divided into three types. The first type is known as the carbonate aggregates. This type includes dolomite and limestone. The second type is the siliceous aggregates. The materials of this type consist of silica. It includes sandstone and granite. The last type is the lightweight aggregates which are produced by heating clay, shale or slate [1]. Different types of aggregates react differently when exposed to high temperature and the mechanical and thermal properties of these aggregates and the cement paste makes them respond differently to high temperatures. Cement paste may expand or shrink based on either its thermal expansion or moisture loss is controlling. These differences in physical characteristics between the cement paste and aggregates make them deform differently which leads to cracks around the aggregate particles. When concrete is subjected to high temperature, it will first lose some of its strength. However, as the temperature increases, concrete starts to gain strength and may exceed itsoriginal strength at 100-200 °C. After that, the strength of concrete will decrease with further increase in temperature [2]. High temperature can also affect shrinkage, creep, porosity, and can result in weight loss of concrete. Moreover, one of the major problems that concrete faces when it is exposed to high temperature is spalling. Spalling is the ablation of pieces and layers of concrete due to high and rapid increase in temperature [2]. For Normal Strength Concrete, spalling occurs when concrete is exposed to a temperature increase at the rate of 20°C/min [3]. But the risks are higher with High Strength Concrete (HSC), due to its low porosity, explosive spalling may occur in HSC as the pressure build up inside the concrete. For HSC, spalling can occur at a temperature increase rate of less than 5°C/min [4]. The factors influencing spalling are: Moisture Content, Water/Cement ratio, Permeability, Heating condition, Concrete strength, Mix proportions, Section size, Reinforcement, Cover, Density, and Applied load [2]. In addition, there are many types of spalling such as Explosive Spalling which occurs early within the first 30 minutes at temperatures around 200-300°C, Surface Spalling, Aggregate Splitting, Corner Separation, Sloughing off, and Post Cooling Spalling [2].

Effect of High Temperature on Steel Bars

As what was mentioned before, steel is affected more by high temperature than concrete. The effect of high temperature on the properties of steel is associated with the type of reinforcement. The yield strength of hot-rolled steels is maintained up to 420°C, and for the cold-drawn steel it can maintain its strength for 260°C, so the rate of resisting high temperatures is associated with pre-stressed and non-pre-stressed concrete elements [1].

Effect of High Temperature on the Bond between Concrete and Steel Reinforcement

Under high temperature, the bond between the steel bars and concrete will be reduced or even lost. This happens due to the difference in deformation between the two materials. The thermal expansion coefficient of concrete at 400°C is about 20 x 10-6/°C. This value may vary based on the type of aggregates used in the concrete mixture. However, the thermal expansion coefficient of steel at 400°C is about 13 x 10-6/°C. This difference in the coefficient of thermal expansion between the two materials results in a progressive damage in the interface between them which leads to a loss in the bond strength [2]. Moreover, the type of bars used in concrete contributes to amount of bond strength lost at high temperatures. There were four conducted experiments showed that the bond strength was reduced by 40% for rounded steel bars at a temperature of 200°C. In addition, the bond strength of deformed steel bars was only reduced by 15% [2]. Also, the curing conditions may contribute to the bond strength at high temperatures. Moist curing was found to have less bond strength than dry curing at temperatures below 400°C [2].

ACI 216 Method

This is a standard containing design and analytical procedures. It aims to determine the fire resistance associated with concrete and masonry elements and also building assemblies through calculation procedures. The procedures related to the determination for the requirements for the concrete cover, protecting columns of structural steel by the use of concrete or masonry, and others are provided in this standard [5].

Remarks

After the literature review was studied, it was concluded that high temperatures have negative effects on all components of reinforced concrete and its properties. These effects were considered to be implemented to study the effects of elevated temperatures on designed structural systems of a hotel building. Some of the experimental data founded in the literature review was considered to be used to reflect the effect of elevated temperatures on the structural elements in the structural models.

III. RESEARCH METHODOLOGY

Inputs

1. Obtaining the architectural drawings for the hotel building.
2. Using local and international standards to calculate loads and slab thicknesses for the two different structural systems and also calculating the wall loads according to the architectural drawings.
3. Assuming initial logical dimensions for the beams in the solid slab system, edge beams in the flat slab system, and columns and walls in both systems in order to assign these values in the software (STAAD PRO) for the design purposes.
4. Speechifying certain rooms in the building that have a high probability to cause fires in order to be the source of the high temperature loads
5. Specifying certain structural elements which are beams and columns in order to be studied for the effect of temperature loads.
6. Specifying certain temperature loads and their effects on the properties of concrete and steel which are provided in the literature review to be used in the design models for both systems.

Processes

1. Using a structural analysis and design software (STAAD PRO) to convert the architectural drawings into 3D structural models.
2. Applying the calculated loads on the structures and then analyzing the models.
3. Designing both slab systems on the software (STAAD PRO).
4. Applying the specified temperature loads and their effects on the properties of concrete and steel on the specified rooms for both structural systems at different times.

Outputs

1. Reporting the structural design for both slab systems.
2. Reporting the studied effects of high temperature loads and their effects on the properties of concrete and steel for both slab systems. This includes the change on the required area of steel for different structural elements as well as the change on the moments and axial forces for different structural elements.

Codes Used for Structural Design

1. Saudi Building Code for Loading "SBC 301": used to calculate Dead Load, Live Load, Roof Live Load, Wind Load and Seismic Load [6].
2. Building Code Requirements for Structural Concrete (ACI 318-14): used to calculate the slab thickness for both structural systems [7].

IV. PARAMETERS USED FOR ANALYSIS AND DESIGN

Overview

The general properties of materials used in the design of both structural systems were considered to be the same. The concrete was considered to be a normal weight concrete having a compressive strength (f'c) of 25 MPa. The reinforcing steel was considered to be Grade 60 having a yield tensile strength (fy) of 420 MPa.

Calculations of Loads

The loadings that were considered in the design of the structural systems included:

1. Dead Loads (DL), which included self-weight, floor finishing and wall loads..
2. Live Loads (LL), which was obtained from SBC 301.
3. Seismic Loads (SL), which was obtained from the seismic loading maps in the SBC 301.
4. Wind Loads (WL), which was obtained from the SBC 301.
5. High Temperature Loads, which was obtained from the literature review.
6. Roof Live Load (Lr), which was obtained from the SBC 301.

Loading combinations that were considered for the design of the structural systems were based on SBC 301. Temperature Loads were considered to be implemented in the material properties according to the relations found in the literature review.

Calculations of Slab Thickness

Slab thicknesses were calculated according ACI 318 [7]. The structural drawings were studied carefully in order to determine the required thickness for each slab system. The determination of the required thickness is associated with the critical slabs. These slabs have long spans in one or two directions. Long

spans require higher thicknesses to avoid the defection of slabs. It was essential to find the critical one-way solid slab, two-way solid slab and the flat slab. The adopted thickness for the solid slab system is 200 mm. The adopted thickness for the flat slab system is 250 mm.

Specified Temperatures and Material Properties Used for Studying the Effect of Elevated Temperatures

In order to study the effect of elevated temperatures on the structural systems, it is essential to have certain data related to conducted researches in this area such as the ones provided in the literature review. This study aimed to determine the effect of elevated temperatures on the maximum shear force, bending moment and deflection for different structural elements. To study this effect, it was considered to use some the data found on the literature review that includes the changes in the compressive strength and modulus of elasticity of concrete. The effect of high temperatures on the compressive strength and modulus of elasticity of concrete was taken from Bilow et al. [1]. The assumed type of aggregate was considered to be siliceous aggregate. Moreover, the assumed initial values of the compressive strength and modulus of elasticity of concrete, not subjected to the high temperatures, were taken to be 25 MPa and 2107.18 MPa, respectively. These values were reduced according to the reduction percentages of the initial values provided in the charts. Table 1 summarizes the specified temperatures and material properties used to study the effect of elevated temperatures on structural systems.

Table 1: Specified Temperatures and Material Properties Used to Study the Effect of Elevated Temperatures on Structural Systems

Type of Temperature Load	Difference in Temperature (0C)	f'c (MPa)	Ec (MPa)
No Effect of Temperature		25	21,718.00
Ambient Temperature	30	23.75	21,718.00
Elevated Temperature	200	22.5	15,202.60
	400	21.88	10,859.00
	600	12.5	4,343.60

V. STRUCURAL MODELING

Design of Structural Systems

Design of Solid Slab System

The dimensions of the structural elements were increased several times until no failure occurred in the structural elements. The final dimensions that satisfy the function of the structure are the following:

1. The thickness of slabs is 0.2 m.
2. The dimensions of the cross-sectional area of beams having lengths ranging from 7 to 10 m are (0.8 m x 0.4 m).
3. The dimensions of the cross-sectional area of columns having a height of 3.3 m are (0.6 m x 0.6 m) and (0.7 m x 0.7 m).
4. The thickness of shear walls is 0.4 m.

Figs 1 and 2 show the obtained designs of a beam and a column for the solid slab system, respectively.

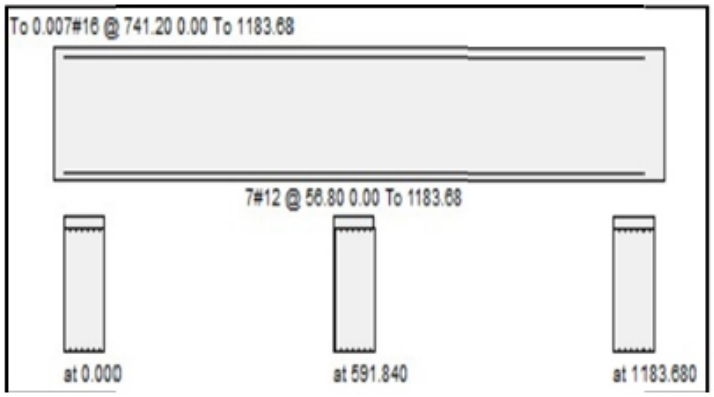

Fig.1. Obtained Design of a Beam for the Solid Slab System.

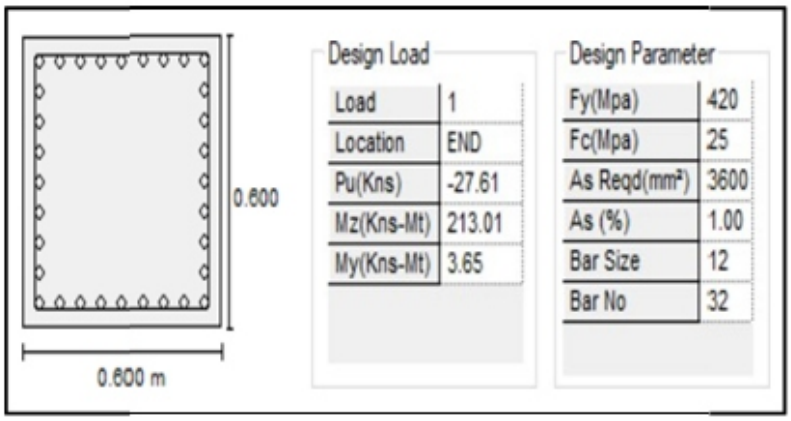

Fig.2. Obtained Design of a Column for the Solid Slab System.

5.1.2. Design of Flat Slab System

The dimensions of the structural elements were increased several times until no failure occurred in the structural elements. The final dimensions that satisfy the function of the structure are the following:

1. The thickness of slabs is 0.25 m.
2. The dimensions of the cross-sectional area of edge beams having lengths ranging from 7 to 10 m are (0.55 m x 0.4 m) and (0.65 x 0.45).
3. The dimensions of the cross-sectional area of columns having a height of 3.3 m are (0.5 m x 0.5 m), (0.6 m x 0.6 m) and (0.7 m x 0.7m).
4. The thickness of shear walls is 0.4 m.

Figs 3 and 4 show the obtained designs of an edge beam and a column for the flat slab system, respectively.

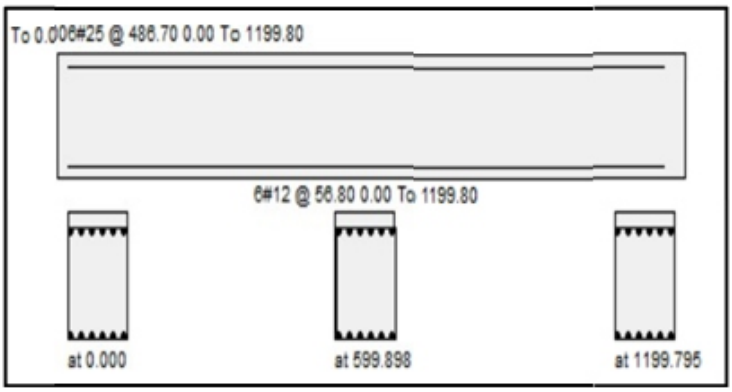

Fig.3. Obtained Design of an Edge Beam for the Flat Slab System.

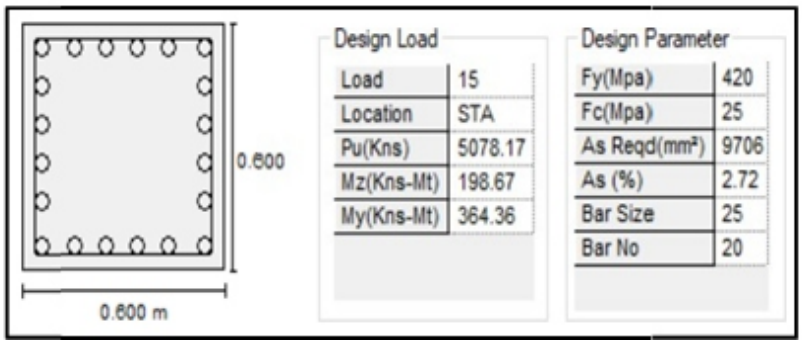

Fig.4. Obtained Design of a Column for the Flat Slab System.

The Study of the Effect of Elevated

Temperatures on the Structural Systems

The summarized data on Table 1 was assigned to the STAAD PRO on separate models depending on the temperature difference. It was used to analyze how the change in the temperature difference may affect both systems. It was considered that the mechanical and electrical rooms are the ones having a high pro ability to cause fires. Therefore, the effect of emperature loads and their associated effects on the pro erties of concrete and steel were assigned to different structural elements subjected to the high temperatures. The main output of this study was to determine the change in the moments, axial forces and the required area of steel for different structural elements which were columns and beams. Fig 5 shows the locations in the building where the effect of high temperature loads and their associated changes in the properties of concrete and steel were applied. The areas having the blue color are the ones having a high probability to cause fire which are the mechanical and electrical rooms.

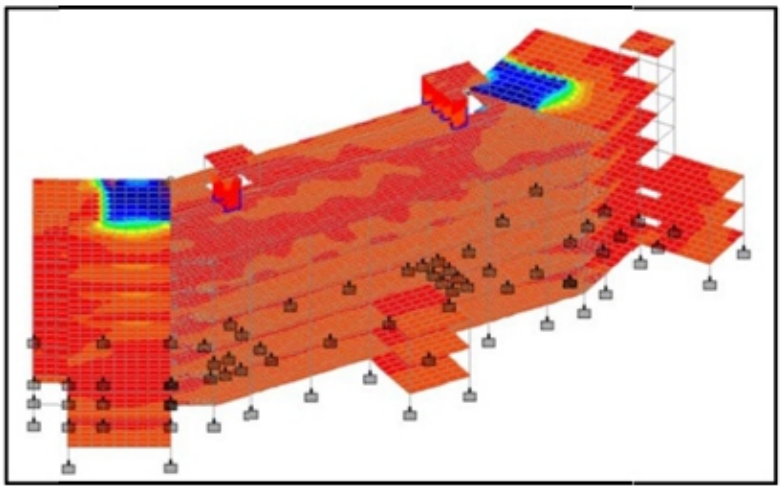

Fig.5. Locations in the Building Having a High Probability to Cause Fire.

Fig 6 shows the beams that were considered in the study. Beams 1 and 2 were subjected to the high temperatures which are 200, 400 and 600 ^{0}C. In addition, beams 1 and 3 were subjected to the ambient temperature which was 30 ^{0}C. In addition, Fig 7 shows the columns that were considered in the study. Column 1 was subjected only to the ambient temperature which is 30 ^{0}C. Columns 2 and 3 were subjected to the high temperatures which are 200, 400 and 600 ^{0}C. Column 4 was considered because it is located near the source of high temperatures.

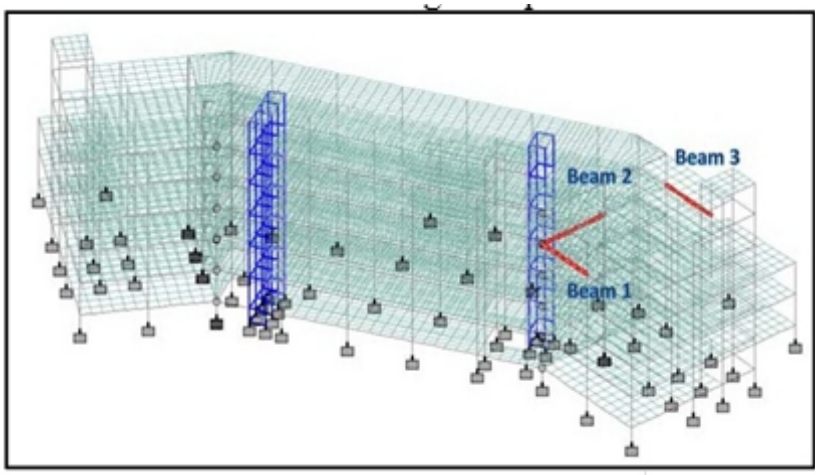

Fig.6. Beams Considered in the Study

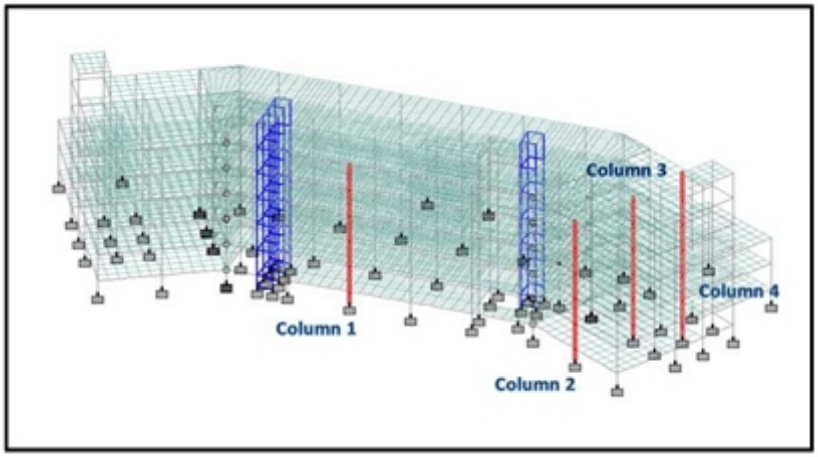

Fig.7. Columns Considered in the Study

The Effect of Elevated Temperatures on the Solid Slab Beams

The effect of temperature loads on the beams of the solid slab system was determined by recording the change in the required area of steel. It was essential to record these values without temperature loads in order to have a benchmark for the required area of steel.

Table 2 shows the specified material properties and the obtain results for the beams that were considered in the study without temperature loads. The specified material properties based on Table 1 include the Compressive Strength of Concrete (f'_c) and the Modulus of Elasticity of Concert (E_c).The obtained results include Required Area of Steel of the Beam without the Effect of High Temperatures (A_c). Tables 3 through 6 show the specified material properties and the obtain results for the beams that were considered in the study with temperature loads of 30, 200, 400, and 600 ^{0}C. The obtained results are the Required Area of Steel of the Beam for the Effect of High Temperatures (A_r), and the ratio between A_r and A_c.

Table 2: Required Area of Steel for Solid Slab Beams without Temperature Load

Beam NO.	Dimension(m)	f'c (MPa)	Ec (MPa)	A_c (mm^2)
1	0.4x0.55	25	21718.5	821
2		25	21718.5	902
3		25	21718.5	708

Table 3: Change in Required Area of Steel for Solid Slab Beams with a Temperature Load of 30 ^{o}C

Beam NO.	Dimension (m)	f'c (MPa)	Ec (MPa)	A_r (mm^2)	A_r/Ac
1	0.4x0.55	23.75	21718.5	821	1
2		23.75	21718.5	902	1
3		25	21718.5	708	1

Table 4: Change in Required Area of Steel for Solid Slab Beams with a Temperature Load of 200 ^{0}C

Beam NO.	Dimension (m)	f'c (MPa)	Ec (MPa)	A_r (mm^2)	A_r/Ac
1	0.4x0.55	22.5	15202	2859	3.48
2		22.5	15202	2666	2.96
3		25	21718.5	728	1.03

Table 5: Change in Required Area of Steel for Solid Slab Beams with a Temperature Load of 400 ^{o}C

Beam NO.	Dimension (m)	f'c (MPa)	Ec (MPa)	A_r (mm^2)	A_r/Ac
1	0.4x0.55	21.88	10859	4431	5.4
2		21.88	10859	4013	4.45
3		25	21718.5	745	1.05

Table 6: Change in Required Area of Steel for Solid Slab Beams with a Temperature Load of 600 ^{o}C

Beam NO.	Dimension (m)	f'c (MPa)	Ec (MPa)	A_r (mm^2)	A_r/Ac
1	0.4x0.55	12.5	4343.6	2521	3.07
2		12.5	4343.6	2223	2.46
3		25	21718.5	778	1.10

Based on the previous obtained results of the solid slab beams, the change in the required area of steel in beams with the change in temperature loads was summarized graphically in order to visualize the behavior of these beams at different temperatures. Fig 8 summarizes the change in the required are of steel at different temperature loads.

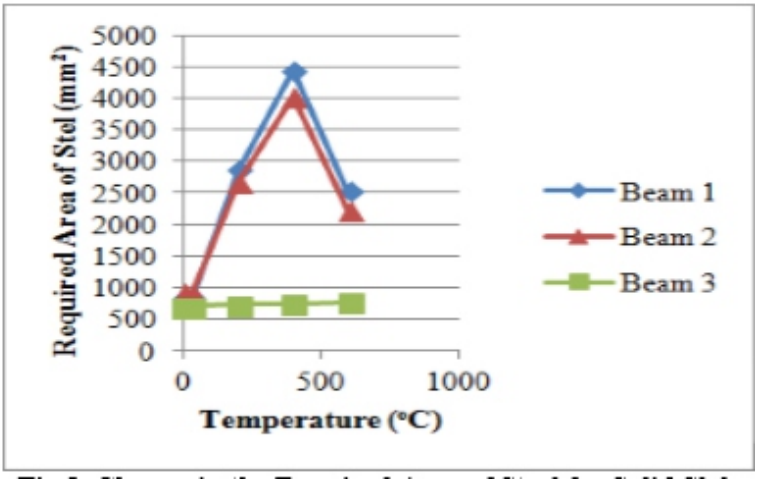

Fig.8. Change in the Required Area of Steel for Solid Slab Beams at Different Temperature Loads.

According to Fig 8, it was observed that the required area of steel was increased with the increase in the temperature load up to 400 oC. At 600 oC there was a decrease in the required area of steel at beams 1 and 2 whereas it has increased in beam 3 as a result of the redistribution of stresses caused by the sharp drop in the modulus of elasticity.

The Effect of Elevated Temperatures on the Solid Slab Columns

The effect of temperature loads on the columns of the solid slab system was determined by recording the change in the area of steel. It was also essential to record these values without temperature loads in order to have a benchmark for the required area of steel. Table 7 shows the specified material properties and the obtain results for the columns that were considered in the study without temperature loads. The specified material properties based on Table 1 include (f'c) and (Ec).The obtained results include the Required Area of Steel for Columns without the Effect of High Temperatures (Ac). Tables 8 through 11 show the specified material properties and the obtain results for the columns that were considered in the study with temperature loads of 30, 200, 400, and 600^{0}C. However, the obtained results are the Required Area of Steel for the Column for the Effect of Temperatures (Ar), and the ratio between Ar and Ac.

Table 7: Required Area of Steel for Solid Slab Columns without Temperature Load

Column No.	Dimension (m)	f'c (MPa)	Ec (MPa)	A_c (mm^2)
1	0.5x0.5	25	21718.5	10548
2	0.6x0.6	25	21718.5	13643
3	0.5x0.5	25	21718.5	14296
4	0.5x0.5	25	21718.5	3600

Table 8: Change in Required Area of Steel for Solid Slab Columns with a Temperature Load of 30 ^{o}C

Column No.	Dimension (m)	f'c (MPa)	Ec (MPa)	A_r (mm^2)	A_r/A_c
1	0.5x0.5	23.75	21718.5	14479	1.37
2	0.6x0.6	23.75	21718.5	16010	1.17
3	0.5x0.5	25	21718.5	14329	1.00
4	0.5x0.5	25	21718.5	3600	1.00

Table 9: Change in Required Area of Steel for Solid Slab Columns with a Temperature Load of 200 ^{o}C

Column No.	Dimension (m)	f'c (MPa)	Ec (MPa)	A_r (mm^2)	A_r/A_t
1	0.5x0.5	25	21718.5	10548	1.00
2	0.6x0.6	22.5	15202	26484	1.94
3	0.5x0.5	22.5	15202	11265	0.79
4	0.5x0.5	25	21718.5	3600	1.00

Table 10: Change in Required Area of Steel for Solid Slab Columns with a Temperature Load of 400 ^{o}C

Column No.	Dimension (m)	f'c (MPa)	Ec (MPa)	A_r (mm^2)	A_r/A_c
1	0.5x0.5	25	21718.5	10548	1.00
2	0.6x0.6	21.88	10859	0	0.00
3	0.5x0.5	21.88	10859	0	0.00
4	0.5x0.5	25	21718.5	3600	1.00

Table 11: Change in Required Area of Steel for Solid Slab Columns with a Temperature Load of 600 ^{o}C

Column No.	Dimension (m)	f'c (MPa)	Ec (MPa)	A_r (mm^2)	A_r/A_c
1	0.5x0.5	25	21718.5	10548	1.00
2	0.6x0.6	12.5	4343.6	0	0.00
3	0.5x0.5	12.5	4343.6	7178	0.50
4	0.5x0.5	25	21718.5	3600	1.00

Based on the previous obtained results of the solid slab columns, the change in the required area of steel in columns with the change in temperature loads was summarized graphically in order to visualize the behavior of these columns at different temperatures. Fig 9 summarizes the change in the required are of steel at different temperature loads for the columns.

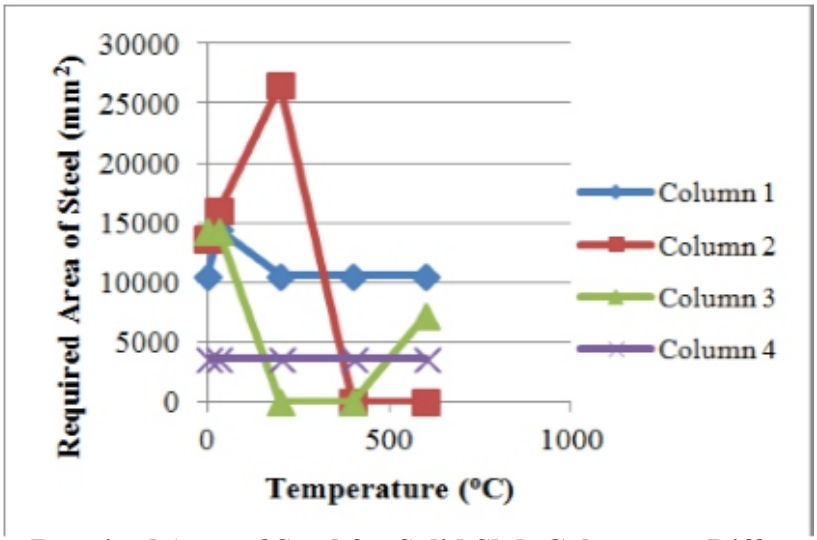

Fig.9. Change in the Required Area of Steel for Solid Slab Columns at Different Temperature Loads.

According to Fig 9, it was observed that at a temperature load of 30 oC, the required area of steel for columns 1 and 2 increased slightly since they were directly subjected to the temperature load.

Moreover, at a temperature load of 200 oC, the required area of steel for Column 2 increased dramatically because it was also subjected directly to the temperature load. However, there was no proper bar arrangement was possible for column 3. At a temperature load of 400 oC, there was no proper bar arrangement was possible for column 2. In addition, at 600 oC temperature load, there was redistribution in stresses in column 3 due to the high reduction in the compressive strength and modulus of elasticity which leaded to an increase in the required area of steel. The required area of steel for column 1 was not affected due to the expansion joints that prevent the transformation of temperature loads.

The Effect of Elevated Temperatures on the Flat Slab Edge Beams

The effect of temperature loads on the edge beams of the flat slab system was determined by also recording the change in the required area of steel. Table 12 shows the specified material properties and the obtain results for the edge beams that were considered in the study without temperature loads. The specified material properties based on Table 1 include also (f'c) and (Ec).The obtained results include (Ac). Tables 13 through 16 show the specified material properties and the obtain results for the beams that were considered in the study with temperature loads of 30, 200, 400, and 600 ^{o}C. The obtained results of these temperature loads are also (Ar) as well as the ratio between Ar and Ac.

Table 12: Required Area of Steel for Flat Slab Edge Beams without Temperature Load

Beam NO.	Dimension (m)	f'c (MPa)	Ec (MPa)	A_c (mm^2)
1	0.4x0.55	25	21718.5	750
2		25	21718.5	649
3		25	21718.5	648

Table 13: Change in Required Area of Steel for Flat Slab Edge Beams with a Temperature Load of 30 ^{o}C

Beam NO.	Dimension (m)	f'c (MPa)	Ec (MPa)	A_r (mm^2)	A_r/A_c
1	0.4x0.55	23.75	21718.5	648	0.86
2		23.75	21718.5	601	0.93
3		25	21718.5	544	0.84

Table 14: Change in Required Area of Steel for Flat Slab Edge Beams with a Temperature Load of 200 ^{o}C

Beam NO.	Dimension (m)	f'c (MPa)	Ec (MPa)	Ar (mm^2)	A_r/A_c
1	0.4x0.55	22.5	15202	1605	2.14
2		22.5	15202	1947	3.00
3		25	21718.5	648	1.00

Table 15: Change in Required Area of Steel for Flat Slab Edge Beams with a Temperature Load of 400 ^{o}C

Beam NO.	Dimension (m)	f'c (MPa)	Ec (MPa)	Ar (mm^2)	A_r/A_c
1	0.4x0.55	21.88	10859	2448	3.26
2		21.88	10859	2910	4.48
3		25	21718.5	648	1.00

Table 16: Change in Required Area of Steel for Flat Slab Edge Beams with a Temperature Load of 600 ^{0}C

Beam NO.	Dimension (m)	f'c (MPa)	Ec (MPa)	A_r (mm^2)	A_r/A_c
1	0.4x0.55	12.5	4343.6	1383	1.844
2		12.5	4343.6	1563	2.40832
3		25	21718.5	648	1

Based on the previous obtained results of the flat slab edge beams, the change in the required area of steel in edge beams with the change in temperature loads was summarized graphically. Fig 10 summarizes the change in the required are of steel at different temperature loads.

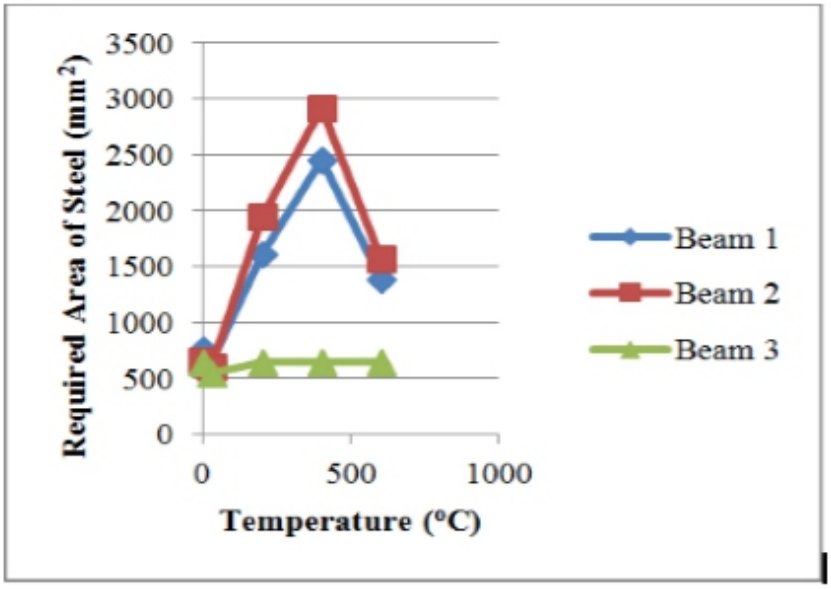

Fig.10. Change in the Required Area of Steel for Flat Slab Edge Beams at Different Temperature Loads.

According to Fig 10, it was observed that the required area of steel was increased with the increase in the temperature load up to 400 oC. At 600 oC there was a decrease in the required area of steel at beams 1 and 2 whereas it has increased in beam 3 as a result of the redistribution of stresses caused by the sharp drop in the modulus of elasticity.

The Effect of Elevated Temperatures on the Flat Slab Columns

The effect of temperature loads on the columns of the flat slab system was also determined by recording the change in the required area of steel. These values were recorded without temperature loads for the benchmark purpose of the required area of steel. Table 17 shows the specified material properties and the obtain results for the columns that were considered in the study without temperature loads. The specified material properties based on Table 1 include (f'c) and (Ec).The obtained results include (Ac). Tables 18 through 21 show the specified material properties and the obtain results for the columns that were considered in the study with temperature loads of 30, 200, 400, and 600 ^{o}C. The obtained results are (Ar), and the ratio between Ar and Ac.

Table 17: Required Area of Steel for Flat Slab Columns without Temperature Load

Column No.	Dimension (m)	f'c (MPa)	Ec (MPa)	A_c (mm^2)
1	0.5x0.5	25	21718.5	13902
2	0.6x0.6	25	21718.5	9706
3	0.5x0.5	25	21718.5	14313
4	0.5x0.5	25	21718.5	3035

Table 18: Change in Required Area of Steel for Flat Slab Columns with a Temperature Load of 30 ^{o}C

Column No.	Dimension (m)	f'c (MPa)	Ec (MPa)	A_r (mm^2)	A_r/A_c
1	0.5x0.5	23.75	21718.5	16586.7	1.19
2	0.6x0.6	23.75	21718.5	12794	1.32
3	0.5x0.5	25	21718.5	14735	1.03
4	0.5x0.5	25	21718.5	2500	0.82

Table 19: Change in Required Area of Steel for Flat Slab Columns with a Temperature Load of 200 ^{o}C

Column No.	Dimension (m)	f'c (MPa)	Ec (MPa)	A_r (mm^2)	A_r/A_c
1	0.5x0.5	25	21718.5	13892	1
2	0.6x0.6	22.5	15202	15041	1.55
3	0.5x0.5	22.5	15202	19995.8	1.4
4	0.5x0.5	25	21718.5	2840	0.94

Table 20: Change in Required Area of Steel for Flat Slab Columns with a Temperature Load of 400 ^{o}C

Column No.	Dimension (m)	f'c (MPa)	Ec (MPa)	A_r (mm^2)	A_r/Ac
1	0.5x0.5	25	21718.5	13888	1
2	0.6x0.6	21.88	10859	26834	2.76
3	0.5x0.5	21.88	10859	0	0
4	0.5x0.5	25	21718.5	2840	0.94

Table 21: Change in Required Area of Steel for Flat Slab Columns with a Temperature Load of 600 ^{o}C

Column No.	Dimension (m)	f'c (MPa)	Ec (MPa)	A_r (mm^2)	A_r/A_c
1	0.5x0.5	25	21718.5	14007	1.01
2	0.6x0.6	12.5	4343.6	17849	1.84
3	0.5x0.5	12.5	4343.6	16809.6	1.17
4	0.5x0.5	25	21718.5	2840	0.94

Based on the previous obtained results of the flat slab columns, the change in the required area of steel in columns with the change in temperature loads was summarized graphically. Fig 11 summarizes the change in the required are of steel at different temperature loads for the columns.

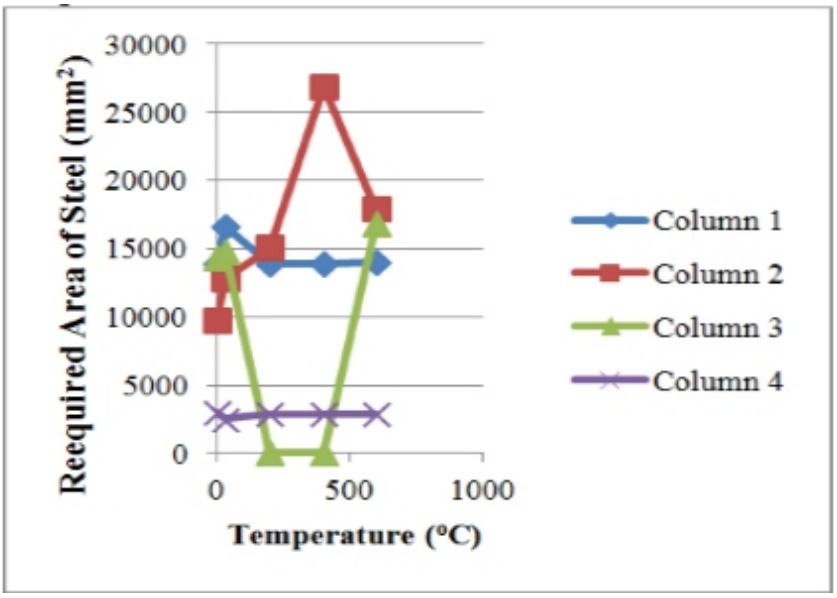

Fig.11. Change in the Required Area of Steel for Flat Slab Columns at Different Temperature Loads.

According to Fig 11, it was observed that at a temperature load of 30 oC, the required area of steel for columns 1 and 2 increased slightly since they were directly subjected to the temperature load. Moreover, at a temperature load of 200 oC, the required area of steel for Column 2 increased because it was also subjected directly to the temperature load. However, there was no proper bar arrangement was possible for column 3. At a temperature load of 400 oC, the required area of steel continued to increase for column 2. In addition, at 600 oC temperature load, there was redistribution in stresses in column 3 due to the high reduction in the compressive strength and modulus of elasticity which leaded to an increase in the required area of steel. The required area of steel for column 1 was not affected due to the expansion joints that prevent the transformation of temperature loads.

VI. CONCLUSIONS AND RECOMMENDATIONS

Concluding Remarks

The following points summarized the conclusion of this study:

1. Specific conducted research experiments related to the effect of elevated temperatures on the reinforced concrete structures were reviewed and studied in order to use some of the obtained experimental data on the designed structural models.
2. Both structural systems were designed based on local and international standards which are the Saudi Building Code for Loading "SBC 301" and the Building Code Requirements for Structural Concrete (ACI 318-11).
3. Both structural systems were analyzed and designed using STAAD PRO. The obtained design having no temperature load was considered to be a benchmark for studying the effect of elevated temperatures on both structural systems.
4. The obtained results were based on recording the change in the required area of steel for specified selected structural elements at different locations. The effect of the redistribution of stresses was

observed for both structural systems at very high temperatures. The location of the structural element and type of temperature load were found to be major factors affecting the redistribution of the stresses and converted structures from safe to unsafe.

5. For the beams of both of solid and flat slabs, it was observed that the required area of steel was increased with the increase in the temperature load up to 400 oC. At 600 oC there was a decrease in the required area of steel at beams 1 and 2 which are located near the mechanical and electrical rooms whereas it has increased in beam 3 as a result of the redistribution of stresses caused by the sharp drop in the modulus of elasticity.
6. For slid slab columns, it was observed that at a temperature load of 30 oC, the required area of steel for columns 1 and 2 increased slightly since they were directly subjected to the temperature load. Moreover, at a temperature load of 200 oC, the required area of steel for Column 2 increased dramatically because it was also subjected directly to the temperature load. However, there was no proper bar arrangement was possible for column 3. At a temperature load of 400 oC, there was no proper bar arrangement was possible for column 2. In addition, at 600 oC temperature load, there was redistribution in stresses in column 3 due to the high reduction in the compressive strength and modulus of elasticity which leaded to an increase in the required area of steel. The required area of steel for column 1 was not affected due to the expansion joints that prevent the transformation of temperature loads.
7. For flat slab columns, it was observed that at a temperature load of 30 oC, the required area of steel for columns 1 and 2 increased slightly since they were directly subjected to the temperature load. Moreover, at a temperature load of 200 oC, the required area of steel for Column 2 increased because it was also subjected directly to the temperature load. However, there was no proper bar arrangement was possible for column 3. At a temperature load of 400 oC, the required area of steel continued to increase for column 2. In addition, at 600 oC temperature load, there was redistribution in stresses in column 3 due to the high reduction in the compressive strength and modulus of elasticity which leaded to an increase in the required area of steel. The required area of steel for column 1 was not affected due to the expansion joints that prevent the transformation of temperature loads.

RECOMMENDATIONS

1. Different structural design and construction methods can be considered for this structure such as precast concrete. These structures can be subjected to the temperature loads in order to determine their behavior.
2. Designers should take into account the effect of temperature loads (at least ambient temperature loads in order to avoid cracks).

ACKNOWLEDGMENTS

The authors would like to express their gratitude to King Fahd University of Petroleum and Minerals (KFUPM) for facilitating conducting research.

REFERENCES

[1] D. N. Bilow, O. O. Road, M. E. Kamara, and O. Road, "Fire and Concrete Structures," in Structure Congress 2008, 2008, no. 1.

[2] K. Willam, Y. Xi, K. Lee, and B. Kim, "Thermal Response of Reinforced Concrete Structures in Nuclear Power Plants," 2009.

[3] G. A. Khoury, "Effect of fire on concrete and concrete structures," Prog. Struct. Eng. Mater., pp. 429–447, 2000.

[4] L. T. Phanl, J. R. Lawson, and F. L. David, "Effects of elevated temperature exposure on heating characteristics, spalling, and residual properties of high performance concrete," Mater. Struct., vol. 34, no. March, pp. 83–91, 2001.
[5] ACI/TMS Committee 216, Code Requirements for Determining Fire Resistance of Concrete and Masonry Construction Assemblies. Farmington Hills, M: American Concrete Institute, 2014.
[6] SBC National Committee 301, Saudi Building Code Structural requirements for Loads and Forces (SBC 301). Saudi Building Code, 2007.
[7] ACI Committee 318, Building Code Requirements for Structural Concrete (ACI 318-14). Farmington Hills, MI: American Concrete Institute, 2014.

Modeling and Analysis of Optimized Rectangular RC Columns Confined with CFRP Composites

[1]Rajai Z. Al- Rousan, [2]Khairedin M. Abdalla, [3]Mohammad A. Alhassan, [4]Nikos D. Lagaros

[1,2,3]Department of Civil Engineering, Jordan University of Science & Technology, Jordan
[4]Department of Structural Engineering, National Technical University Athens (NTUA)
E-mail: [1]rzalrousan@just.edu.jo, [2]abdalla@just.edu.jo, [3]maalhassan@just.edu.jo,
[4]nlagaros@central.ntua.gr

A B S T R A C T

The structural behavior of rectangular reinforced concrete (RC) columns confined with different configurations of carbon fiber reinforcement polymers (CFRP) sheets is investigated by using nonlinear finite element analysis (NLFEA). SOLID65, LINK8, SOLID45, and SOLID46 elements represented the concrete, steel bars, steel plates, and CFRP sheets, respectively. Based on each simulated component's actual characteristics, the nonlinear material properties are defined for each type of elements. The NLFEA results clearly confirmed that the use of CFRP composites strengthening system for RC columns improves the ductility and ultimate axial strength capacity. The enhancement in the ductility and axial strength increased with the increasing of the number of CFRP composite layers. The CFRP composite strengthening system of rectangular RC columns can be categorized as efficient and successful only if significant increase in the ultimate axial strength capacity is achieved. As confirmed by the results of this study, NLFEA can efficiently simulate the structural behavior of rectangular RC columns confined with CFRP sheets. It is recommended that the NLFEA model can be used in additional research studies to develop design guidelines and rules for RC structural elements strengthened with CFRP composites.

Keywords - NLFEA, CFRP, Simulation, RC Columns.

I. INTRODUCTION

Strengthening, repairing and seismic retrofitting of reinforced concrete (RC) structures with Carbon Fiber Reinforced Polymer (CFRP) composites has become enormously promising composite materials due to its light weight, high strength, and ease of application. There are many engineering strengthening applications in which CFRP was externally bonded onto the surface of RC elements to improve their ductility and strength [1-4]. In order to better understand the mechanical mechanism, the behavior of confined RC columns with CFRP sheets needs further investigated. Modeling of the complex nonlinear behavior of RC rectangular column is a challenge in the FEA of structural concrete elements. Therefore, few researchers attempted to simulate the behavior of RC externally strengthened with FRP composites using FEA [5-15]. In this study, the ANSYS finite element program [16] was used to simulate the behavior and the effectiveness of various configurations of CFRP confinement of the rectangular RC columns. Actual geometry and steel reinforcing details of experimentally tested rectangular column specimens as well as the used strengthening configuration and the number of the externally bonded CFRP layers were considered in the NLFEA. The load-deflection response, load- strain response, and failure mode were obtained for each specimen by the NLFEA and compared to the companion experimental test results.

II.FINITE ELEMENT ANALYSIS

Element SOLID65 was used to model the concrete material without steel reinforcing bars. The element is capable to crack in three orthogonal directions, crush, creep, and plastically deforms [16]. The ultimate uniaxial tensile strength of 4.5 MPa, compressive strength of 55 MPa, and initial young's modulus (Ec) =35063 MPa are needed to define a failure surface for the concrete. As a result, William and Warnke (1975) [17] was used to defined the concrete criterion for failure of the concrete due to a multiaxial stress state as shown in Figure 1(a). Also, Poisson's ratio of 0.2 shear transfer coefficient (bt) of 0.2 [18] were used in this study.

A 3-D spar element (LINK8) was used to model the steel bars with a uniaxial tension-compression behavior and is also capable of plastic deformation [16]. An elastic-perfectly plastic material is assumed for steel which is identical in tension and compression as shown in Fig. 1(b). The Poisson's ratio and steel yield stress are 0.3 and 413 MPa. A SOLID45 (eight-node solid element) was used for the supports and load application steel plates [16] to provide an even stress distribution over the support and loading areas. A linear elastic material with an elastic modulus equal to 200 GPa and Poisson's ratio of 0.3 were assumed for steel plates. Finally, layered element (SOLID46) was used to model the CFRP composite sheet which has orthotropic material properties in each layer [16] with a thickness of 0.165 mm, elastic modulus of 228 GPa, tensile strength of 4275 MPa, and ultimate tensile strain of 0.017 mm/mm in the fibers direction. Firstly, the quarter of the column was simulated to study the behavior by taking benefit of symmetry of the column geometry and loading with proper boundary conditions which reduces the computer disk space requirements and computing time. At both column ends, one end was modeled as pin support while the translation and rotation in the loading direction were only allowed at the other column end. In order to determine the appropriate mesh density (Fig. 2), a convergence study was carried out.

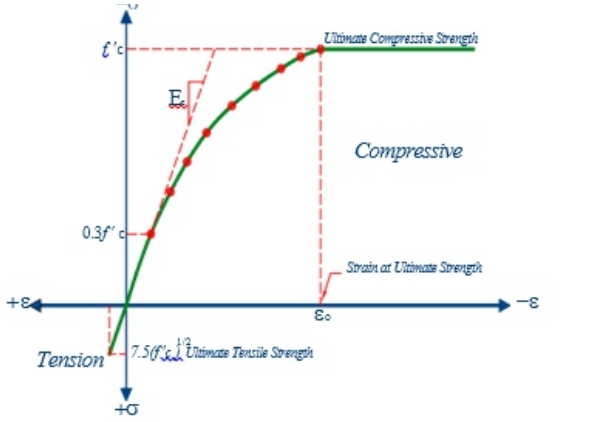

(a) Concrete

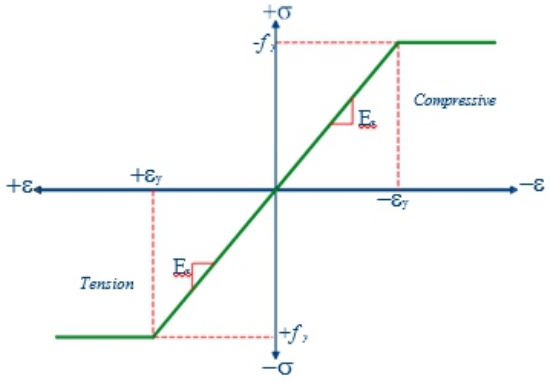

(b) Steel reinforcement

Fig. 1 Stress-Strain curve

Perfect bonding between the concrete and steel reinforcement as well as between CFRP composite and concrete was assumed. Rectangular RC columns with a length of 750 mm and cross section of 125 mm×150 mm, were simulated in order to model the response of confined rectangular RC columns with various configurations of CFRP sheets under axial loading. All the columns were reinforced longitudinally with 4□10 steel bars and laterally with steel ties of 5 mm diameter at a spacing of 125 mm except at the ends (25 mm spacing), and this is due to the stress concentration at the ends. Also, these critical ends were additionally strengthened with two layers of CFRP composite sheets for a distance of 125 mm. The cross-section, reinforcement details, and the CFRP composite confinement configurations of the columns are shown in Fig. 3. The applied vertical load was divided up to failure into a series of small load increments of 0.45 kN. Convergence at the end of each load increment was checked by using Newton-Raphson equilibrium iterations. Failure of each column model was identified when the solution for a vertical load increment of 0.0045 kN was not converging.

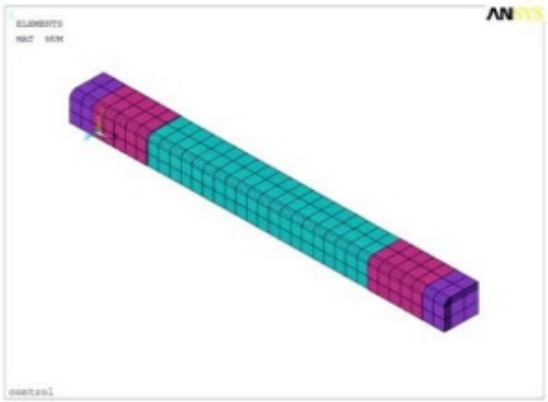

(a) Quarter of the column

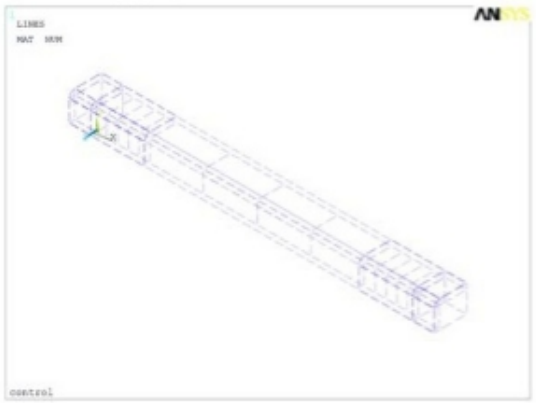

(b) Steel reinforcement

Fig. 2 Typical finite element meshing quarter of the column

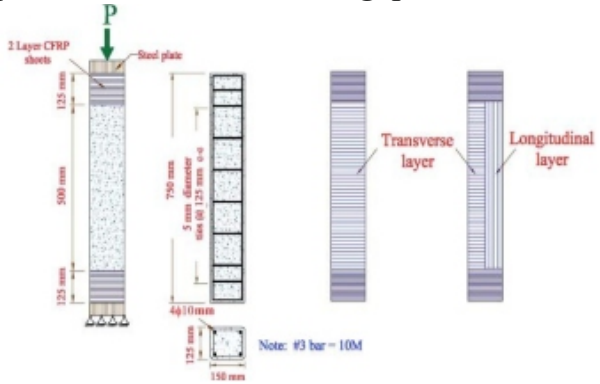

Fig. 3 Cross section and reinforcement details

III. RESULTS AND DISCUSSION

A. Load-Displacement Response

The characteristics of the CFRP confined columns were evaluated based on the load-displacement behavior. Fig. 4 shows the NLFEA axial load versus axial displacement curves of the simulated columns. The ultimate loads were 1072, 1588, 1659, 1757, 1817, 1912, 1968, and 2046 kN as shown in Table 1. The corresponding increase in the ultimate axial load with respect to the control specimens was 48%, 55%, 64%, 70%, 78%, 84%, and 90%, respectively. The axial load–displacement curves shown in Fig. 4 reveal that there is a significant increase in the ultimate axial load as well as in the ultimate axial displacement when confining the columns with CFRP sheets. Fig. 4 also shows that the increase in the ultimate loads and displacements is directly related to an increase in the number of CFRP sheet layers.

TABLE I: ANSYS results at ultimate

Confinement Configuration	Ultimate load, kN	Percentage of increase in ultimate load with respect to control specimen (%)
Control (unconfined)	1072	---
1-layer in the transverse direction (1T)	1588	48.1
1-layer in the transverse direction and 1- layer in the longitudinal (1T1L(OUT))	1659	54.8
2-layers in the transverse direction (2T)	1757	63.9
1-layer in the longitudinal and 1-layer in the transverse direction (1T1L(in))	1817	69.5
3-layers in the transverse direction (3T)	1912	78.4
1-layer in the longitudinal and 2-layers in the transverse direction (2T1L(in))	1968	83.6
4-layers in the transverse direction (4T)	2046	90.6

B. Load-Strain Response

The axial and circumferential strains at the critical region of the columns were plotted versus the axial load as shown in Fig. 5. The axial load-axial strain response followed a similar trend as the axial load-axial displacement for each specimen type. At failure, the circumferential strain readings of the confined columns were greater than 0.017 mm/mm, which is the maximum strain capacity of the carbon fiber. The circumferential strain results are coinciding with the observed failure mode of the confined columns, the failures did not occur before the fracturing of the CFRP sheets.

This reveals that the effectiveness of the CFRP confinement was good. Based on the NLFEA results shown in Figs. 4 and 5, it can be observed that confinement of rectangular RC column with CFRP significantly enhances its strength and ductility performance under axial loading. Typical distribution of CFRP sheet and concrete strains at control and confinement columns were shown in Figs. 6-13.

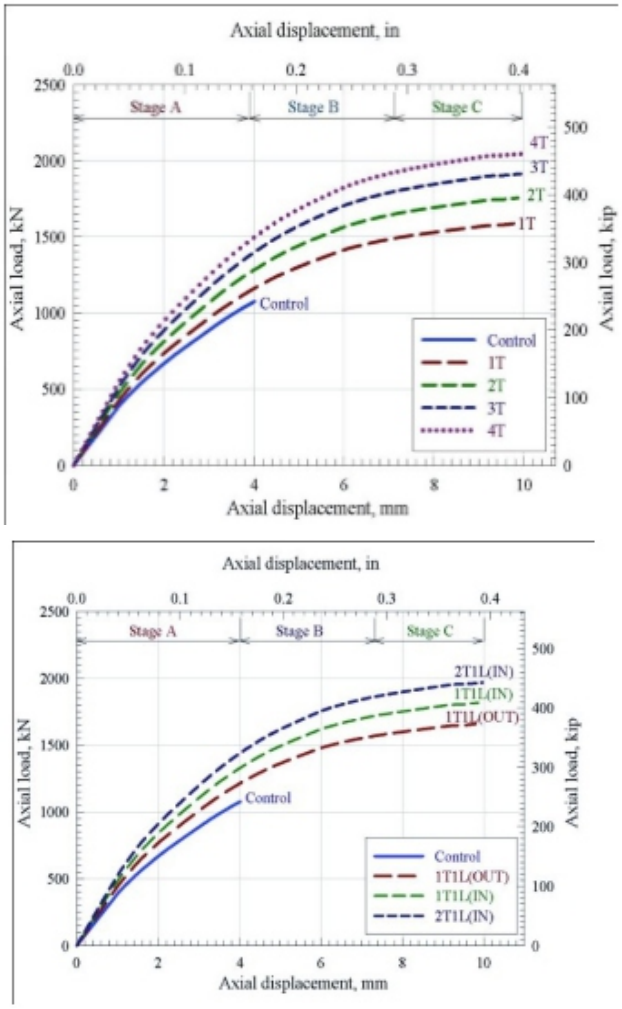

Fig. 4 Axial loads versus axial displacements

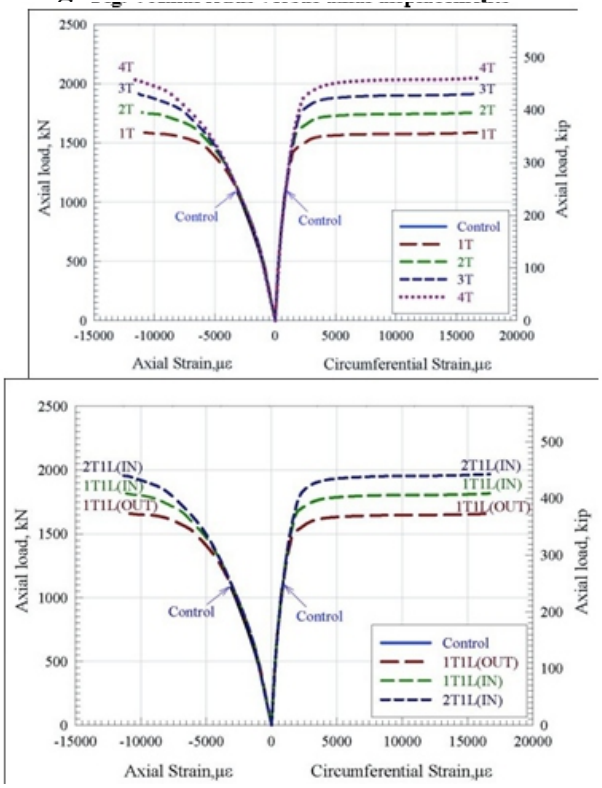

Fig. 5 Axial load versus axial and circumferential strain curves

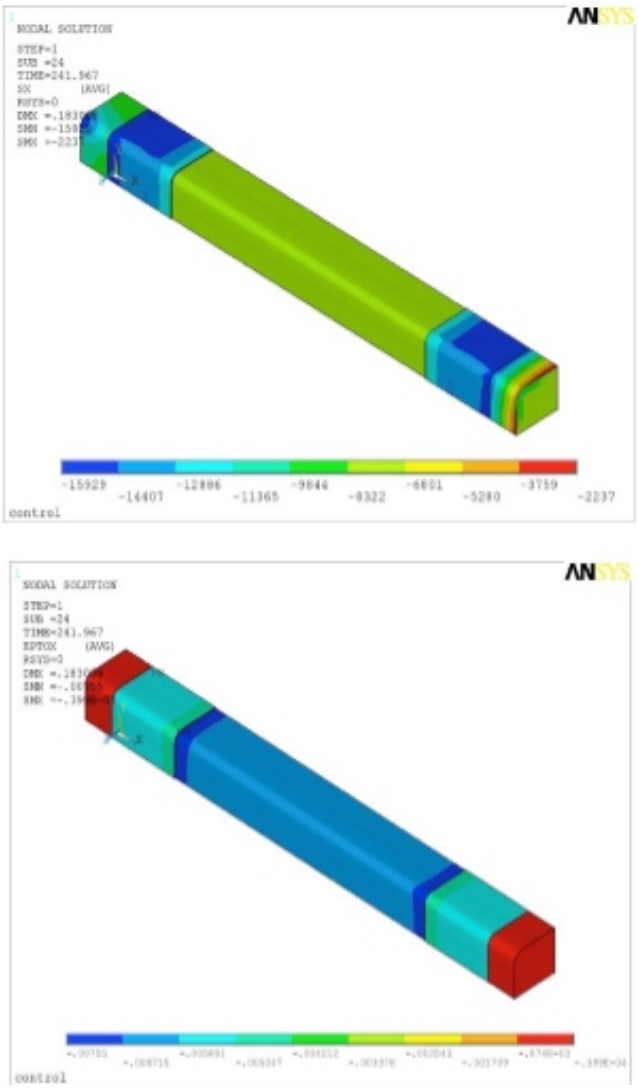

Fig. 6 Strain and stress contours of control column

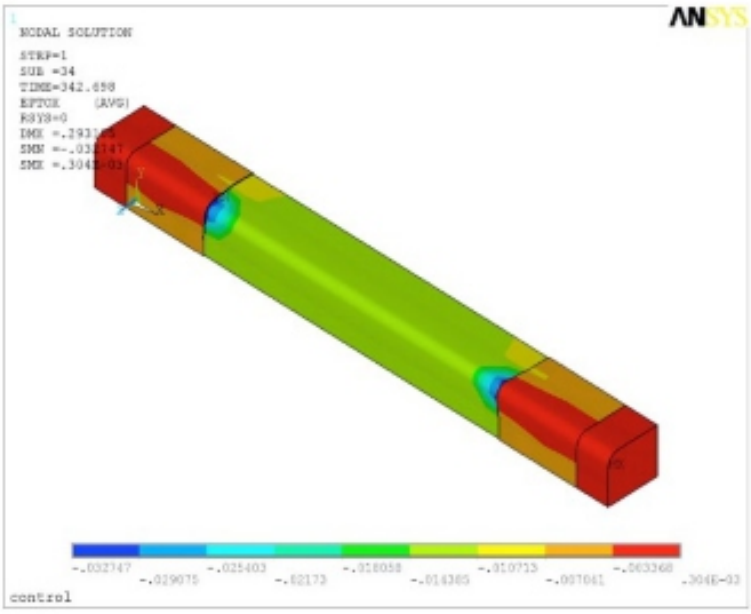

Fig. 7 Strain contours with one layer in the transverse direction

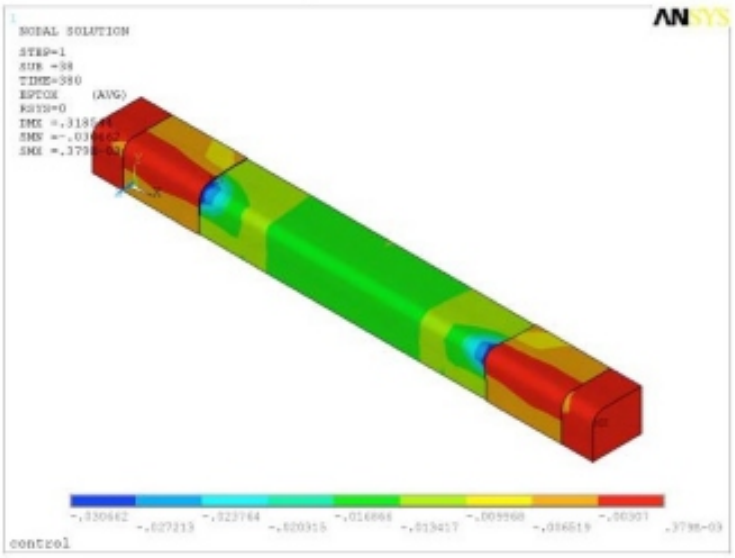

Fig. 8 Strain contours with 2 layers in the transverse direction

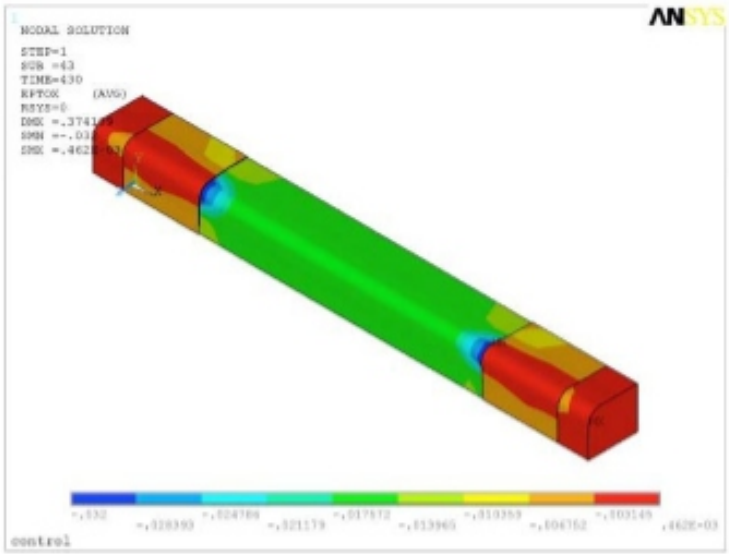

Fig. 9 Strain contours with 3 layers in the transverse direction

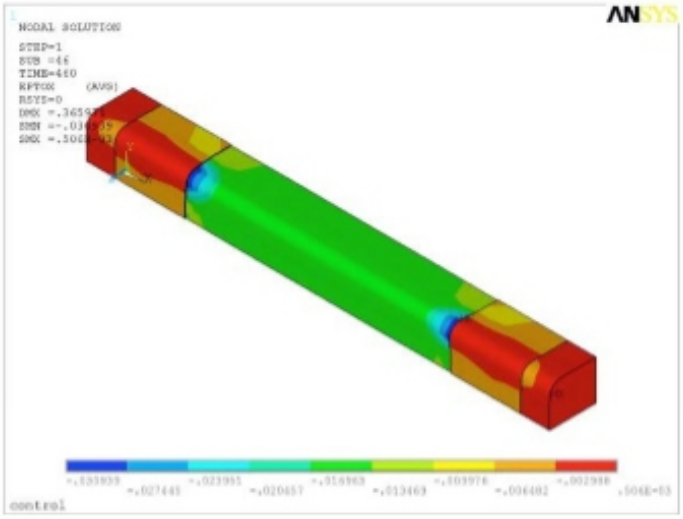

Fig. 10 Strain contours with 4 layers in the transverse direction

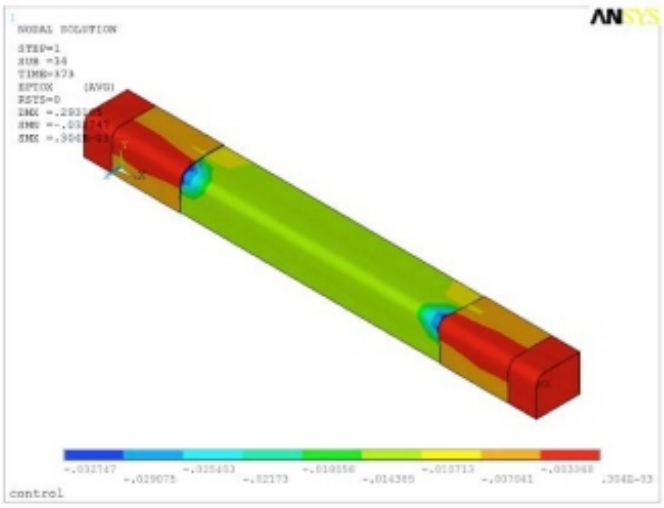

Fig. 11 Strain contours of column with one layer in the longitudinal (out) and one in the transverse direction

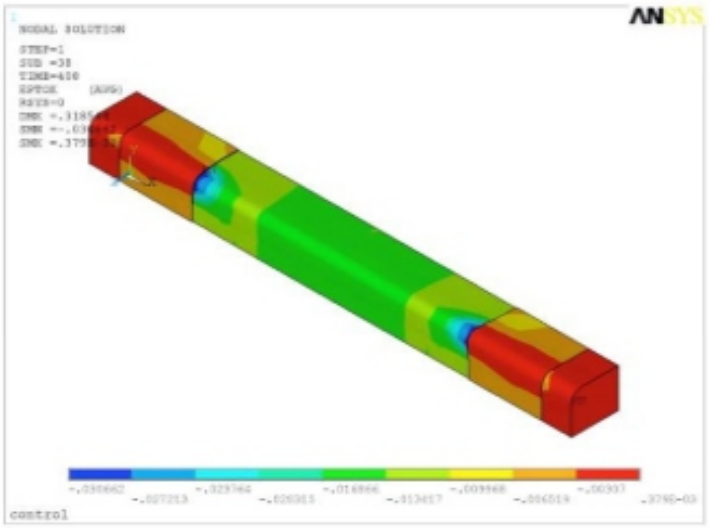

Fig. 12 Strain contours of column with one layer in the longitudinal (in) and one in the transverse direction

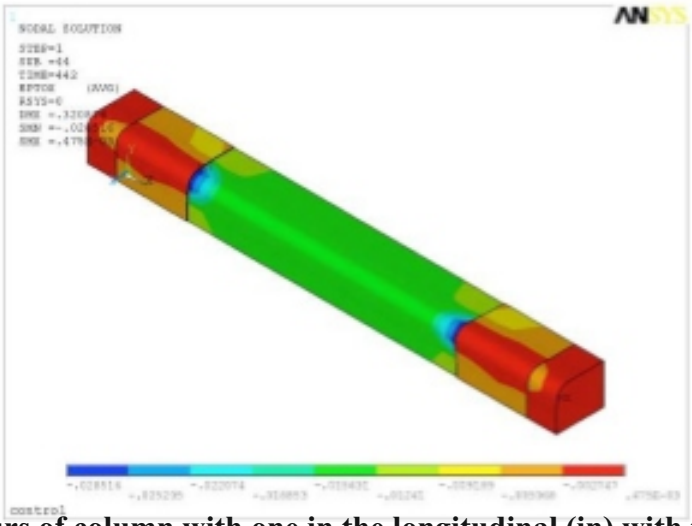

Fig. 13 Strain contours of column with one in the longitudinal (in) with two in the transverse direction

CONCLUSION

Externally bonded CFRP sheets are very effective in enhancing the axial strength and deformation capacity of concrete columns. Increasing the number of CFRP sheet layers leads to a significant increase in the ultimate axial strength and a slight increase in the ultimate displacement. Also, two CFRP sheet layers is the optimum number of CFRP layers and this is based on the load strain behavior. Higher axial loads and strains at failure were recorded for the confined RC columns wrapped with CFRP in comparison with the unconfined ones. This finite element model can be used in additional studies to develop design rules for strengthening RC columns using CFRP composites.

ACKNOWLEDGEMENT

This work has been supported by the OptArch Project – Optimization Driven Architectural Design of Structures – (H2020-Rise-2015). Their support is highly acknowledged. The authors would like also to thank JUST for its support.

REFERENCES

[1] Richart, F. E., Brandtzaeg, A., and Brown, R. L. (1928). "A study of the failure of concrete under combined compressive stresses." Engineering Experiment Station Bulletin No. 185, University of Illinois, Urbana, Illinois.

[2] Saadatmanesh, H., Ehsani, M. R., and Li, M. W. (1994). "Strength and ductility of concrete columns externally reinforced with fiber composite straps." ACI Structural Journal, Vol. 91, No. 4, pp. 434-447.

[3] Issa, M., and Tobaa, H. (1994). "Strength and ductility enhancement in high-strength confined concrete." Magazine of Concrete Research, Vol. 46, No. 168, pp. 177-189.

[4] Picher, F., Rochette, P., and Labossiére, P. (1996). "Confinement of concrete cylinders with CFRP." Proceeding, ICCI'96, Tucson, Ariz., pp. 829-841.

[5] Kachlakev Damian, Miller Thomas, and Yim Solomon. (2001). 'Finite Element Modeling of Reinforced Concrete Structures Strengthened with FRP Laminates' Report for Oregon Department Of Transportation, Salem.

[6] Tedesco,J.W., Stallings J.M., and El-Mihilmy, M.. (1999). 'Finite Element Method Analysis of a Concrete Bridge Repaired with Fiber Reinforced Plastic Laminates', Computers and Structures, pp. 379-407.

[7] P. Feng, X. Z. Lu & L. P. Ye (2002). "Experimental research and finite element analysis of square concrete columns confined by FRP sheets under uniaxial compression", Proceedings of 17th Australasian Conference on the Mechanics of Structures and Materials. Gold Coast, Australia, pp. 60-65.

[8] Al-Rousan, R. Empirical and NLFEA prediction of bond-slip behavior between DSSF concrete and anchored CFRP composites. Construction and Building Materials, Vol. 169, No. 1, 2018, pp. 530-542.

[9] Al-Rousan, R., Alhassan, M., Ababneh, A. Simulating the response of CFRP strengthened shear-keys in composite concrete bridges. Materials and Design, Vol. 90, No. 1, 2016, pp. 733-744.

[10] Al-Rousan, R.Z. Effect of CFRP Schemes on the Flexural Behavior of RC Beams Modeled by Using a Nonlinear Finite-element Analysis. Mechanics of Composite Materials, Vol. 51, No. 4, 2015, pp. 437-446.

[11] Al-Rousan, R., Haddad, R.H., Al Hijaj, M.A., Optimization of the economic practicability of fiber-reinforced polymer (FRP) cable-stayed bridge decks, Bridge Structures, Vol. 10, No. 4, 2014, pp. 129-143.

[12] R. Al-Rousan and R. Haddad, NLFEA Sulfate-damage Reinforced Concrete Beams Strengthened with FRP Composites, Composite Structures Journal, Vol. 96, No. 1, 2013, pp 433-445.

[13] R. Alrousan, M. Issa, and H. Shabila, Performance of reinforced concrete slabs strengthened with different types and configurations of CFRP, Composites Part B: Engineering Journal, Vol. 43, No. 2, 2012, pp 510-521.

[14] R. Alrousan, and M. Issa, Fatigue Performance of Reinforced Concrete Beams Strengthened with CFRP Sheets, Construction and Building Materials Journal, Vol. 25, No. 8, 2011, pp 3520-3529.

[15] Mohsen A. Issa, Rajai Alrousan, and Moussa Issa. Experimental and Parametric Study of Columns with CFRP Composites. Journal of Composites for Construction, ASCE, Vol. (13), No. (2), 2009, pp 135-147.

[16] ANSYS, ANSYS User's Manual Revision 16.0, ANSYS, Inc.

[17] William, K. J. and Warnke, E. P. (1975). "Constitutive Model for the Triaxial Behavior of Concrete," Proceedings, International Association for Bridge and Structural Engineering, Vol. 19, ISMES, Bergamo, Italy, pp. 174.

[18] Hemmaty, Y., (1998). "Modelling of the Shear Force Transferred Between Cracks in Reinforced and Fibre Reinforced Concrete Structures," Proceedings of the ANSYS Conference, Vol. 1, Pittsburgh, Pennsylvania.
[19] ACI 318-05 (2005). American Concrete Institute, "Building Code Requirements for Reinforced Concrete," American Concrete Institute, Farmington Hills, Michigan.
[20] Desayi, P. and Krishnan, S., (1964). "Equation for the Stress- Strain Curve of Concrete," Journal of the American Concrete Inst., 61, pp. 345-350.

Rubble Mound Breakwaters Under Tsunami Attack

C. E. Balas
Gazi University, Faculty of Engineering and Architecture, Civil Engineering Department, Ankara, Turkey.

A B S T R A C T

In the past applications of risk assessment for coastal structures; only wave characteristics, tidal range, storm surge, wave set-up, surf beat and structural system parameters were considered, but the tsunami risk could not be incorporated to the reliability-based design in the literature. The reliability model REBAD introduced in this study primarily enabled the risk assessment of breakwaters subject to tsunami risk. The Second-Order Reliability Method (SORM) was applied to determine the safety of Haydarpaşa Port, Sea of Marmara, Turkey. The failure probability was forecasted by approximating the Van der Meer failure surface with a second-degree polynomial having an equal curvature at the design point. The inclusion of tsunami risk that has an extended return period when compared to storm waves increased the failure risk of the structure in its lifetime. For Haydarpasa port main breakwater, the failure risk of the structure was not sensitive to the tsunami occurrence. However, in places with significant seismic activity, tsunami risk may be very significant depending on the occurrence probability and the magnitude of the tsunami.

I. INTRODUCTION

The safety of coastal structures is evaluated by modeling random resistance and load variables with probability distributions at the limit state. The implementation of REBAD model [1] that can be employed both for design and safety evaluation intentions, to the design of rubble-mound breakwaters has significant importance especially in countries such as Turkey, where the tsunami risk is substantial in Marmara and Aegean regions. REBAD enabled the design to be accomplished for several damage levels and failure consequences, leading to an optimal design where initial and maintenance costs of the structure were optimized [2]. The hydraulic failure mode of the armor layer is described regarding its limit state to compare the effects of failure mode response functions on the preliminary design of rubble-mound breakwaters including tsunami risk [3].

II. STRUCTURAL RISK ASSESSMENT

REBAD deals with the problems of uncertainty that affect most of the variables in structural reliability, since the design of coastal structures incorporates a considerable extent of uncertainty in the resistance and potential load intensities [4]. The safety of the structure relies on the joint influence of loads acting on the structure and the available strength. The limit state function defined for a specific failure mode consists of load and strength variables that are random in nature.

The primary variable vector z in the normalized space indicates these random variables. The serviceability limit-state was implemented for the safety evaluations, as the exceedance of the failure damage level that may not result in complete breakdown of the structure but may cause an interruption in the achievement of its functions. The functional form of the basic variables used in the limit state is defined as failure function by: $g(z)=(z1,z2,...,zn)$. The safety of the structure can be assured by designating an admissible value of the probability of achieving the limit state defined by: $g(z)=0$. The failure probability of the coastal structure Pf, i.e. the probability of reaching the limit state that is

influenced by the uncorrelated extreme value distribution of wave height, can be expressed in universal form:

$$P_f = \int\int\int_{g(Z)=0} \ldots \int f_{Z_1,\ldots,Z_n}(z_1,\ldots,z_n)\,dz_1,\ldots,dz_n \qquad (1)$$

where, fZi (zi) is the joint probability density function of standardized basic variables Zi. For a definite damage level, this failure probability can be comprehended as the exceedance probability of that damage level. In system reliability, the second order estimate to the failure probability is obtained by approaching the joint failure set by the set bounded by hyperplanes at the design point on the joint failure surface closest to the origin [5]. In the applications for a selected design wave, tidal level, storm surge and tsunami set-up were randomly generated (on average 30,000 times) from the probability distributions to obtain the design load of the breakwater. Its reliability was investigated (again on average 30,000 times) by the SORM method at the limit state.

Consequently for each randomly generated load combination of the computer, the joint damage probability reflected both the occurrence probability of loading conditions and the exceedance probability of the limit state which is the damage level of the Haydarpasa main breakwater under tsunami attack.

III. CASE STUDY: HAYDARPASA PORT BREAKWATER

The Haydarpasa port situated on the Anatolian side of the Bosphorus (latitude 41 00 N and longitude 29 01) has a wide hinterland connected to inland using highways and railroads which are the shortest route connecting Europe to Middle East countries. The port has two breakwaters of 1700 m and 600 m long protecting the sea area of 62 hectares. The main breakwater was designed at a depth of 15 m. with armor weights of 4 tonnes on a slope of 1:2.5 (Table 1). The significant design wave height and period were Hs= 4m and Ts=6 sec, respectively, obtained from extreme value statistics [6].

The reliability risk assessment model was applied in order to evaluate the structural safety of the breakwater by modelling random design and structural variables, i.e. wave height, tidal range, storm surge, wave set-up and the structural system parameters by probability distributions (Table 2). The wave set-up and surf beat were taken as 6% and 9% of the significant wave height, respectively [7]. Since the breakwater was constructed at a depth of 15 m tsunami height is taken as the design parameter as defined in Figure (1) [8].

The available information concerning tsunamis associated with the Istanbul and the eastern Marmara earthquakes have been used as the tsunami data [9]. Data documented for Istanbul between the years of 358-1999 (1641 years) gives the number of major tsunamis in Istanbul and on the coasts of Marmara Sea as 32, where the tsunami height exceeds 0.5 m, as descriptively listed in Table (3).

There are several valuable magnitude and intensity definitions, classifications and statistical approaches for the occurrence probabilities of the tsunami. Efforts towards the quantification of the tsunami regarding intensity scale started with Sieberg [10]. Since then several investigators put a great effort to grade the tsunami in terms of intensity [11] and magnitude scales [12] [13] [14] [15] [16] [17]. Based on these studies Table (4) was prepared for structural risk assessment, with the possible tsunami height ranges judged by the intensity scale and the descriptions related to the major earthquakes in the Marmara region tabulated in Table (3) which is adopted from Altinok and Ersoy [9]. With the limited data, the tsunami height ranges were identified based on the tsunami information in Table (3).

The lack of tsunami intensity and magnitude scale with detail description in the data utilized forced the investigators to decide on the tsunami height range by using Modified Sieberg Seismic Sea-Wave Intensity Scale (i) [11] in Table (3). In this table, HTm is the maximum tsunami wave height (m), D is the distance that the water penetrated inland (m) and NTI designates that there is no tsunami information. As a pioneering work, a simple statistical analysis of the classified tsunami heights in Istanbul and the adjacent coasts of Marmara is analyzed regarding the probability of occurrences of the mean values of the ranges as given in Figure (2).

TABLE I. Design parameters for Haydarpaşa main breakwater.

Design Variable X_i	Value
Nominal diameter D_n (m.)	1.15
Weight W_{50} (tones)	4.0
Design wave height H_s (m.)	4.0
Tidal range R_T (m.)	±0.25
Surf Beat (m.)	0.42
Storm surge S_S (m.)	0.22
Relative density Δ_p	1.64
The height of structure (m.)	10
Structure slope Cotθ	2.5

In this figure, the regression line, presenting the statistical characteristic of the mean values, was provided with a certain confidence limit indicating the lowest and the highest tsunami height ranges. The purpose of this attempt was to introduce a simple conceptual, statistical model of tsunami occurrence and the probability distribution of tsunami height for Istanbul. Based on the number of events of tsunamis in 1641 years, the return period of tsunami heights (for the mean values of ranges) were estimated as given in Table (5).

Climatic and geomorphologic changes in the future may alter the statistical characteristics of tsunamis in the Marmara region. Hence it is well known that modeling of the tsunami, in general, depends on the number and accuracy of data, period studied and the statistical analysis techniques utilized. Although this study is based on the limited descriptive data available, results were regarded as representative of the population. The structural performance function g(zi) for the rubble mound breakwater was simulated under design conditions using the probability distributions of the load and strength parameters for the following two cases: Case I: Tsunami risk not included and Case II: Tsunami risk included.

TABLE II. Probability parameters of variables used in reliability-based risk assessment.

X_I	Distribution	Parameters
Y	Beta	a=2.9 ; b=2.1 c=1.4
D_n	Beta	a=3.1 b=1.6 c=1.5
H_s	Gumbel	a=1.88 b=0.78
Tide	Triangular	min=-0.25 max=0.25
Tsunami height	Log-normal	a=2.3 b=8.3
Δ_ρ	Normal	μ_{xi}=1.64 σ_{xi}=0.13
Cotθ	Beta	a=9 ; b=1.8 c=2.8

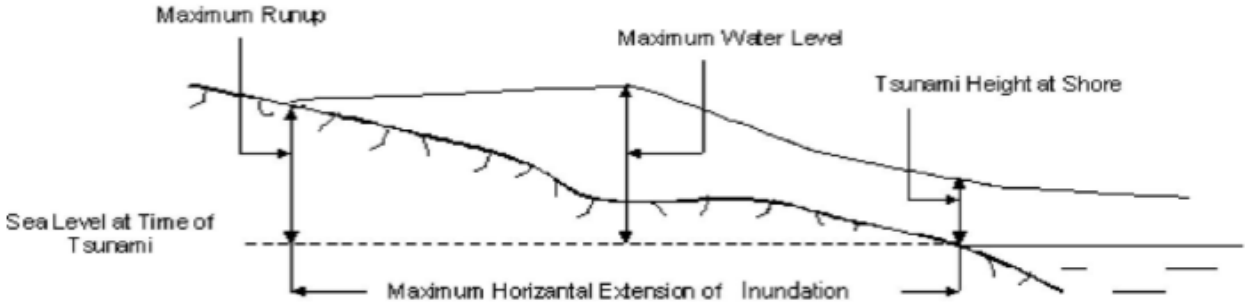

Figure 1. Maximum run-up of tsunami inundation, adopted from Farreras [8].

The scatter range of the randomly generated values was between gmin= –44.2 m and gmax=3.68 m for Case I; gmin=–44.3 m and gmax=3.64 m, for Case II. This signifies the effect of uncertainties inherent in the design parameters of the limit-state functions having the simulated mean values of μg=1.1 m (Case I) and μg=1.08 m (Case II) (Table 6).

Simulation results for Case I and Case II are illustrated in Figure (3a-b), respectively, where the occurrence probability of structural performance function in 100 years is given. From Figure (3-a), where the tsunami risk was not included (Case I), structural performance function g(zi) was safe with an annual probability of 99.95%, signifying that the failure risks will be 1.65% and 3.25% in 50 years and 100 years, respectively.

As for the Case II (Figure 3b) where the tsunami risk was included, it is seen that, the structural performance function is safe with an annual probability of 99.98% signifying the failure risks as 2.2% and 4.2% in 50 years and 100 years, respectively.

It is clearly seen that, including the tsunami risk increased the failure risk of the breakwater and it is observed that:

TABLE III. Major tsunamis in Istanbul and Marmara region,

Date	Place	Tsunami Information
24.08.358	Izmit Gulf, Iznik, Istanbul	NTI
11.10.368	Iznik and its surroundings	NTI
01.04.407	Istanbul	NTI
08.11.447	Marmara Sea, Istanbul, Izmit Gulf, Marmara Islands	i=3
26.01.450	Marmara Sea, Istanbul	i=3
26.09.488	Izmit Gulf	NTI
Winter 529	Thracian coasts of Marmara	NTI
Winter 542	West coast of Thracia	i=4
06.09.543	Kapidag Peninsula, Erdek Bandirma	NTI
15.08.553	Istanbul, Izmit Gulf	D=3000 m.
15/16.08.555	Istanbul, Izmit Gulf	NTI
14.12.557	Istanbul, Izmit Gulf	D=5000 m.
715	Istanbul, Izmit Gulf	NTI
26.10.740	Marmara Sea, Istanbul, Iznik Lake	i=3/i=4
26.19.975	Istanbul, Thracian coast of Marmara	i=3
989	Istanbul, Marmara coast	NTI
990	Istanbul, Marmara coast	NTI
02.02.1039	Istanbul, Marmara coast	NTI
23.09.1064	Iznik, Bandirma, Murefte, Istanbul	NTI
12.02.1332	Marmara Sea, Istanbul	i=3
14.10.1344	Istanbul, Marmara coast, Thracian coast, Gelibolu	i=4
10.09.1509	Istanbul, Marmara coast	i=3 HTm >6m.
17.07.1577	Istanbul	NTI
05.04.1646	Istanbul	i=3/i=4
15.08.1551	Istanbul	NTI
02.09.1554	Izmit Gulf, Istanbul	NTI
22.05.1766	Istanbul, Marmara coast	i=2
23.05.1829	Istanbul, Gelibolu	i=2
19.04.1878	Izmit, Istanbul, Marmara coast	i=3
10.05.1878	Izmit, Istanbul	40 people killed by tsunami
09.02.1894	Istanbul	i=3 HTm <6 m.
18.09.1963	Eastern Marmara, Yalova, Gemlik Gulf	H_{Tm} =1m.
17.09.1999	Izmit Gulf	i=3

TABLE IV. Tsunami height range defined for the structural risk assessment.

Intensity	Tsunami height range	Description
I = very light ii =light	H_T=0.1-1 m.	Minor
iii = rather strong iv = strong	H_T=1-3 m.	Moderate
V= very strong vi =disastrous	H_T=3-6 m.	Major

TABLE V. Return periods based on the number of occurrences of tsunamis in 1641 years.

Tsunami Height (m.)	Return Period (years)
H_T=0.5	R_p=50
H_T=2.0	R_p=100
H_T=4.0	R_p=200

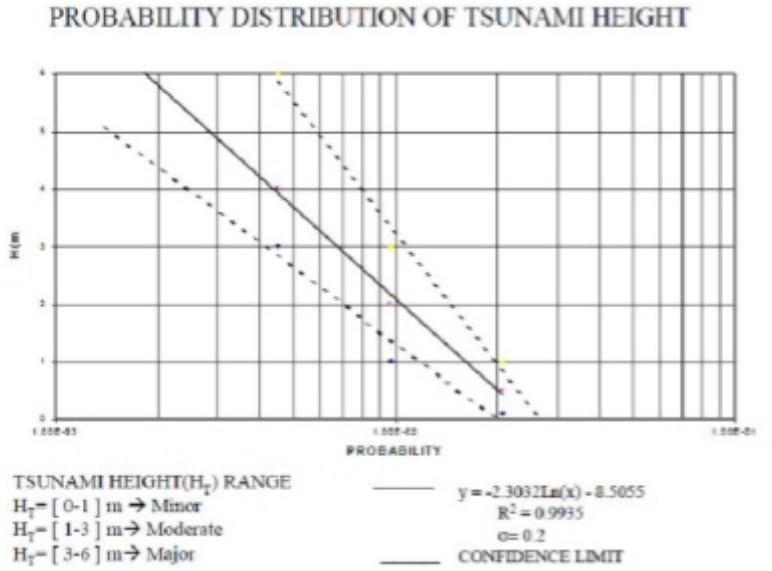

Figure 2. Tsunami heights in Istanbul and the adjacent coasts of Marmara regarding the probability of occurrences of the mean values.

TABLE VI Simulation of failure function for 100 years.

Cases	Tsunami not included	Tsunami risk included
Fitted distribution of g	Gumbel	Gumbel
Distribution parameters	Mode: 1.75 Scale: 0.77	Mode: 1.71 Scale: 0.8
Average (μ_g m.)	1.1	1.08
Minimum of range	-44.2	-44.3
Maximum of range	3.68	3.64

1. The failure probability is relatively higher in Case II (tsunami included) than Case I (not included).
2. Longer years, the failure probability and the impact of tsunami risk on the failure mechanism are increased.

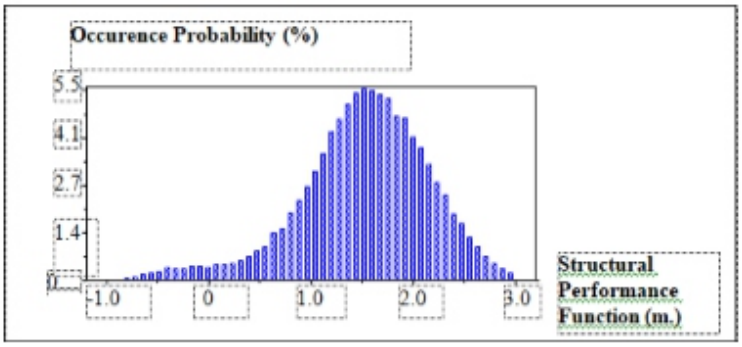

(a)

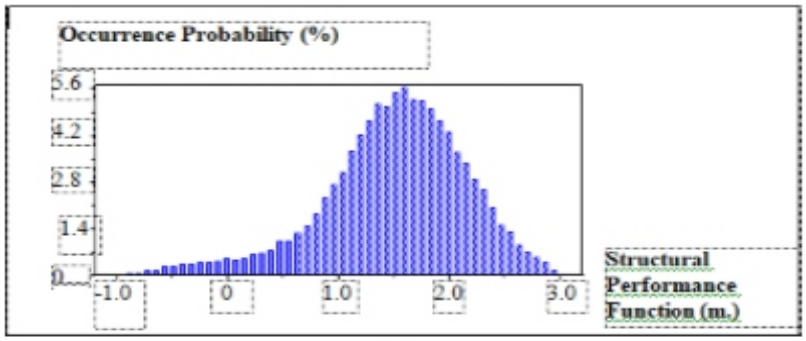

(b)

Figure 3. Distribution of the Van der Meer plunging performance function at the limit state in 100 years. (a) The case I: Tsunami risk not considered (b) Case II: The effect of tsunami risk.

1. For Haydarpasa port main breakwater, the tsunami was not the key design parameter when compared to storm waves. Therefore, the difference in the failure risk was not very significant.
2. However, in places with great seismic activity, tsunami risk may be very significant depending on the occurrence probability and the magnitude of the tsunami.

CONCLUSIONS

The reliability-based structural risk assessment (REBAD) model serves as a basis for risk identification and risk response in coastal projects by integrating time, cost and risk information. In the model, the resistance and load parameters are contemplated as random variables, and the consequences of structural failure are reflected regarding probability distributions by using SORM. The second order estimate to the failure probability is obtained by approaching the joint failure surface by the set bounded by hyperplanes at the design point on the joint failure surface closest to the origin of the coordinate system.

REBAD that can be efficiently utilized for risk assessment of coastal projects in project management permits the coastal engineer to inspect the sensitivity of the structural design to various parameters and contributes a quantitative foundation for comparing design alternatives with assorted damage levels. It provides a valuable tool in the design of coastal structures, which are characterized by large failure consequences and substantial capital expenditures.

The model could incorporate the uncertainties inherent in the tsunami, storm surge and wave data to reliability- based design of rubble mound breakwaters by using Van der Meer performance function. Simulation randomly generated the tidal range of sites and the storm surge.

Afterward, the failure mode probability was predicted by the parabolic limit state surface having the identical curvature at the design point with the higher degree failure surface.

The reliability method had advantages when compared to the deterministic practice since the random behavior of structural performance could be estimated at the planning stages. Therefore, the new reliability approach, which can be applied within few minutes of CPU time in portable computers, was recommended for the design of breakwaters.

Tsunami risk should be included in the reliability- based model since it increased the failure risk as a risk parameter in this case study. Especially in places with high seismic activity, where the magnitude of the tsunami and its occurrence probability is high, tsunami gains vital importance. Such a structural risk assessment, carried out by using reliability-based models, may be used as a successful tool in emergency preparedness and response to natural hazards, as an early risk mitigation mechanism for critical coastal projects, such as nuclear power plants.

REFERENCES

[1] Balas, C.E. and Balas L. (2002) Risk Assessment of Some Revetments in South West Wales, UK, ASCE Journal of Waterway, Port, Coastal and Ocean Engineering, American Society of Civil Engineers, 61 (In print).

[2] Balas, C.E. and A. Ergin (2002) Reliability-Based Risk assessment in Coastal Projects: Case Study in Turkey, ASCE Journal of Waterway, Port, Coastal and Ocean Engineering, American Society of Civil Engineers, 128, No. 2, 52-61.

[3] Balas, C.E. and Koç L. (2002) Risk Assessment of Vertical Wall Breakwaters- A Case Study in Turkey, China Ocean Engineering, 15, No: 4, 453-466.

[4] Balas, C.E., A.T. Williams, S.L. Simmons and A. Ergin (2001), "A Statistical Riverine Litter Propagation Model, Marine Pollution Bulletin, 42, No. 11, 1169-1176.

[5] Balas, C. E. and A. Ergin (2000) A Sensitivity Study for the Second Order Reliability-Based Design Model of Rubble Mound Breakwaters, Coastal Engineering Journal,42, No.1, 57- 86.

[6] Ergin, A. and Özhan, E. (1986). Wave Hindcasting Studies and Determination of Design Wave Parameters for 15 Sea Regions, T. Report No: 35, Coastal Engineering Research Center, Civil Eng. Department, Middle East Technical University, Ankara, Turkey.

[7] Goda, Y. (2000). Random Seas and Design of Maritime Structures, World Scientific Publications, London

[8] Farreras, S.F. (2000). Post-tsunami field surveys procedures: An outline, Natural Hazards, Kluwer Academic Publishers, Dordrecht, 21: 207-214.

[9] Altinok, Y. and Ersoy, S. (2000). Tsunamis observed on and near the Turkish coast, Natural Hazards, Kluwer Academic Publishers, Dordrecht, 21: 185-205.

[10] Sieberg, A. (1927). Geologische, Physikalishe und Angewandte Erdbebenkunde, Verlag von Gustav Fisher, Jena.

[11] Ambraseys, N.N. (1962). Data for the investigation of the seismic sea-waves in the Eastern Mediterranean, Bulletin of Seismological Society of America, 52 (4), 895-913.

[12] Imamura, A. (1942). History of Japanese tsunamis, Kayo-No- Kagaku (Oceanography), 2, 74-80 (in Japanese).

[13] Imamura, A. (1949). Journal of Seismological Society of Japan, 2, 23-28 (in Japanese).

[14] Iiada, K. (1956). Earthquakes accompanied by tsunamis occurring under the sea of the islands of Japan, Journal of Earth Sciences, Nagoya University, 4, 1-43.

[15] Iiada, K. (1970). The generation of tsunamis and the focal mechanism of earthquakes, in Adams, W.M. (ed.), Tsunamis in the Pacific Ocean ,East-Western Centre Press, Honolulu, pp. 3-18.

[16] Abe, K. (1979). Size of great earthquakes of 1837-1974 inferred from tsunami data, Journal of Geophysical Research, 84, B4, 1561-1568.

[17] Shuto N. and Matsutomi H. (1995). Field surveys of the 1993 Hokkaido-Nansei-Oki earthquake tsunami, Pure and Applied Geophysics, 144, 3-4, 649-663.

Instructions for Authors

Essentials for Publishing in this Journal

1 Submitted articles should not have been previously published or be currently under consideration for publication elsewhere.

2 Conference papers may only be submitted if the paper has been completely re-written (taken to mean more than 50%) and the author has cleared any necessary permission with the copyright owner if it has been previously copyrighted.

3 All our articles are refereed through a double-blind process.

4 All authors must declare they have read and agreed to the content of the submitted article and must sign a declaration correspond to the originality of the article.

Submission Process

All articles for this journal must be submitted using our online submissions system. http://enrichedpub.com/ . Please use the Submit Your Article link in the Author Service area.

Manuscript Guidelines

The instructions to authors about the article preparation for publication in the Manuscripts are submitted online, through the e-Ur (Electronic editing) system, developed by **Enriched Publications Pvt. Ltd**. The article should contain the abstract with keywords, introduction, body, conclusion, references and the summary in English language (without heading and subheading enumeration). The article length should not exceed 16 pages of A4 paper format.

Title

The title should be informative. It is in both Journal's and author's best interest to use terms suitable. For indexing and word search. If there are no such terms in the title, the author is strongly advised to add a subtitle. The title should be given in English as well. The titles precede the abstract and the summary in an appropriate language.

Letterhead Title

The letterhead title is given at a top of each page for easier identification of article copies in an Electronic form in particular. It contains the author's surname and first name initial .article title, journal title and collation (year, volume, and issue, first and last page). The journal and article titles can be given in a shortened form.

Author's Name

Full name(s) of author(s) should be used. It is advisable to give the middle initial. Names are given in their original form.

Contact Details

The postal address or the e-mail address of the author (usually of the first one if there are more Authors) is given in the footnote at the bottom of the first page.

Type of Articles

Classification of articles is a duty of the editorial staff and is of special importance. Referees and the members of the editorial staff, or section editors, can propose a category, but the editor-in-chief has the sole responsibility for their classification. Journal articles are classified as follows:

Scientific articles:

1. Original scientific paper (giving the previously unpublished results of the author's own research based on management methods).

2. Survey paper (giving an original, detailed and critical view of a research problem or an area to which the author has made a contribution visible through his self-citation);

3. Short or preliminary communication (original management paper of full format but of a smaller extent or of a preliminary character);

4. Scientific critique or forum (discussion on a particular scientific topic, based exclusively on management argumentation) and commentaries. Exceptionally, in particular areas, a scientific paper in the Journal can be in a form of a monograph or a critical edition of scientific data (historical, archival, lexicographic, bibliographic, data survey, etc.) which were unknown or hardly accessible for scientific research.

Professional articles:

1. Professional paper (contribution offering experience useful for improvement of professional practice but not necessarily based on scientific methods);
2. Informative contribution (editorial, commentary, etc.);
3. Review (of a book, software, case study, scientific event, etc.)

Language

The article should be in English. The grammar and style of the article should be of good quality. The systematized text should be without abbreviations (except standard ones). All measurements must be in SI units. The sequence of formulae is denoted in Arabic numerals in parentheses on the right-hand side.

Abstract and Summary

An abstract is a concise informative presentation of the article content for fast and accurate Evaluation of its relevance. It is both in the Editorial Office's and the author's best interest for an abstract to contain terms often used for indexing and article search. The abstract describes the purpose of the study and the methods, outlines the findings and state the conclusions. A 100- to 250-Word abstract should be placed between the title and the keywords with the body text to follow. Besides an abstract are advised to have a summary in English, at the end of the article, after the Reference list. The summary should be structured and long up to 1/10 of the article length (it is more extensive than the abstract).

Keywords

Keywords are terms or phrases showing adequately the article content for indexing and search purposes. They should be allocated heaving in mind widely accepted international sources (index, dictionary or thesaurus), such as the Web of Science keyword list for science in general. The higher their usage frequency is the better. Up to 10 keywords immediately follow the abstract and the summary, in respective languages.

Acknowledgements

The name and the number of the project or programmed within which the article was realized is given in a separate note at the bottom of the first page together with the name of the institution which financially supported the project or programmed.

Tables and Illustrations

All the captions should be in the original language as well as in English, together with the texts in illustrations if possible. Tables are typed in the same style as the text and are denoted by numerals at the top. Photographs and drawings, placed appropriately in the text, should be clear, precise and suitable for reproduction. Drawings should be created in Word or Corel.

Citation in the Text

Citation in the text must be uniform. When citing references in the text, use the reference number set in square brackets from the Reference list at the end of the article.

Footnotes

Footnotes are given at the bottom of the page with the text they refer to. They can contain less relevant details, additional explanations or used sources (e.g. scientific material, manuals). They cannot replace the cited literature.
The article should be accompanied with a cover letter with the information about the author(s): surname, middle initial, first name, and citizen personal number, rank, title, e-mail address, and affiliation address, home address including municipality, phone number in the office and at home (or a mobile phone number). The cover letter should state the type of the article and tell which illustrations are original and which are not.

Address of the Editorial Office:

Enriched Publications Pvt. Ltd.
S-9,IInd FLOOR, MLU POCKET,
MANISH ABHINAV PLAZA-II, ABOVE FEDERAL BANK,
PLOT NO-5, SECTOR -5, DWARKA, NEW DELHI, INDIA-110075,
PHONE: - + (91)-(11)-45525005

Note